25 Haywood, M. E., Hogarth, M. B., Slingsby, J. H., Rose, S. J., Allen, P. J., Thompson, E. M., Maibaum, M. A. et al., Identification of intervals on chromosomes 1, 3, and 13 linked to the development of lupus in BXSB mice. *Arthtitis Rheum.* 2000. **43**: 349–355.

26 Morel, L., Rudofsky, U. H., Longmate, J. A., Schiffenbauer, J. and Wakeland, E. K., Polygenic control of susceptibility to murine systemic lupus erythematosus. *Immunity* 1994. **1**: 219–229.

27 Jørgensen, T. N., Alfaro, J., Enriquez, H. L., Jiang, C., Loo, W. M., Atencio, S., Gubbels Bupp, M. R. et al., Development of murine lupus involves the combined genetic contribution of the *SLAM* and *FcγR* intervals within the *Nba2* autoimmune susceptibility locus. *J. Immunol.* 2010. **184**: 775–786.

28 Lin, Q., Xiu, Y., Jiang, Y., Tsurui, H., Nakamura, K., Kodera, S., Ohtsuji, M. et al., Genetic dissection of the effects of stimulatory and inhibitory IgG Fc receptors on murine lupus. *J. Immunol.* 2006, **177**: 1646–1654.

29 Tsao, B. P., Lupus susceptibility genes on human chromosome 1. *Int. Rev. Immunol.* 2000. **19**: 319–334.

30 Whitmer, K. J., Romball, C. G. and Weigle, W. O., Induction of tolerance to human γ-globulin in FcRγ- and FcγRII-deficient mice. *J. Immunol.* 1997. **159**: 644–649.

31 Engel, P., Eck, M. J. and Terhorst, C., The SAP and SLAM families in immune responses and X-linked lymphoproliferative disease. *Nat. Rev. Immunol.* 2003. **3**: 813–821.

32 Heszei, M., Detre, C., Rietdijk, S. T., Munos, P., Romero, X., Berger, S. B., Calpe, S. et al., A novel isoforms of the Ly108 gene ameliorates murine lupus. *J. Exp. Med.* 2011. **208**: 811–822.

33 Komori, H., Furukawa, H., Mori, S., Ito, M. R., Terada, M., Zhang, M-C., Ishii, N. et al., A signal adaptor SLAM-associated protein regulates spontaneous autoimmunity and Fas-dependent lymphoproliferation in MRL-*Fas*^{lpr} lupus mice. *J. Immunol.* 2006. **175**: 395–400.

34 Fukuyama, H., Nimmerjahn, F. and Ravetch, J. V., The inhibitory Fcγ receptor modulates autoimmunity by limiting the accumulation of immunoglobulin G$^+$ anti-DNA plasma cells. *Nat. Immunol.* 2005. **6**: 99–106.

35 Pritchard, N. R., Cutler, A. J., Uribe, S., Chadban, S. J., Morley, B. J. and Smith, K. G., Autoimmune-prone mice share a promoter haplotype associated with reduced expression and function of the Fc receptor FcγRII. *Curr. Biol.* 2000. **10**: 227–230.

36 Xiang, Z., Cutler, A. J., Brownlie, R. J., Fairfax, K., Lawlor, K. E., Severinson, E., Walker, E. U. et al., FcγRIIb controls bone marrow plasma cell persistence and apoptosis. *Nat. Immunol.* 2007. **8**: 419–429.

37 Yuasa, T., Kubo, S., Yoshino, T., Ujike, A., Matsumura, K., Ono, M., Ravetch, V. J. et al., Deletion of Fcγ receptor IIB renders H-2^b mice susceptible to collagen-induced arthritis. *J. Exp. Med.* 1999.**189**: 187–194.

38 Kleinau, S., Martinsson, P. and Heyman, B., Induction and suppression of collagen-induced arthritis is dependent on distinct Fcγ receptors. *J. Exp. Med.* 2000. **191**: 1611–1616.

39 Johansson, A. C. M., Sundler, M., Kjellén, P., Johannesson, M., Cook, A., Lindqvist, A-K. B., Nakken, B. et al., Genetic control of collagen-induced arthritis in a cross with NOD and C57BL/10 mice is dependent on gene regions encoding complement factor 5 and FcγRIIb and is not associated with loci controlling diabetes. *Eur. J. Immunol.* 2001. **31**: 1847–1858.

40 Chu, E. B., Hobbs, M. V., Ernst, D. N. and Weigle, W. O., In vivo tolerance induction and associated cytokine production by subsets of murine CD4$^+$ T cells. *J. Immunol.* 1995. **154**: 4909–4914.

41 Murphy, E. D. and Roths, J. B., A Y chromosome associated factor in strain BXSB producing accelerated autoimmunity and lymphoproliferation. *Arthritis Rheum.* 1979. **22**: 1188–1194.

42 Moll, T., Martinez-Soria, E., Santiago-Raber, M. L., Amano, H., Pihlgren-Bosch, M., Marinkovic, D. and Izui, S., Differential activation of anti-erythrocyte and anti-DNA autoreactive B lymphocytes by the Yaa mutation. *J. Immunol.* 2005. **174**: 702–709.

43 Pisitkun, P., Deane, J. A., Difilippantonio, M. J., Tarasenko, T., Satterthwaite, A. B. and Bolland, S., Autoreactive B cell responses to RNA-related antigens due to *TLR7* gene duplication. *Science* 2006. **312**: 1669–1672.

44 Subramanian, S., Tus, K., Li, Q., Wang, A., Tian, X. H., Zhou, J., Liang, C. et al., A Tlr7 translocation accelerates systemic autoimmunity in murine lupus. *Proc. Natl. Acad. Sci. USA* 2006. **103**: 9970–9975.

45 Deane, J. A., Pisitkun, P., Barrett, R. S., Feigenbaum, L., Town, T., Ward, J. M., Flavell, R. A. et al., Control of Toll-like receptor 7 expression is essential to restrict autoimmunity and dendritic cell proliferation. *Immunity* 2007. **27**: 801–810.

46 Heidari, Y., Bygrave, A E., Rigby, R. J., Rose, K. L., Walport, M. J., Cook, H. T., Vyse, T. J. et al., Identification of chromosome intervals from 129 and C57BL/6 mouse strains linked to the development of systemic lupus erythematosus. *Genes Immun.* 2006. **7**: 592–599.

47 Davis, R. S., Dennis, G., Jr., Odom, M. R., Gibson, A. W., Kimberly, R. P., Burrows, P. D. and Cooper, M. D., Fc receptor homologs: newest members of a remarkably diverse Fc receptor gene family. *Immunol. Rev.* 2002. **190**: 123–136.

48 Davis, R. S., Stephan, R. P., Chen, C. C., Dennis, G., Jr., and Cooper,M. D., Differential B cell expression of mouse Fc receptor homologs. *Int. Immunol.* 2004. **16**: 1343–1353.

49 Dietrich, W., Katz, H., Lincoln, S. E., Shin, H. S., Friedman, J., Dracopoli, N. C. and Lander, E. S., A genetic map of the mouse suitable for typing intraspecific crosses. *Genetics* 1992. **131**: 423–447.

50 Manly, K. F. and Olson, J. M., Overview of QTL mapping software and introduction to map manager QT. *Mamm. Genome* 1999. **10**: 327–334.

Abbreviations: **BGG:** bovine γ globulin · **B6:** C57BL/6 · **DBGG:** deaggregated BGG · **DHGG:** deaggregated HGG · **FcγRIIB:** IgG Fc receptor IIB · **HGG:** human γ globulin · **LOD:** logarithm of odds · **NZB:** New Zealand Black · **NZW:** New Zealand White · **QTL:** quantitative trait loci · **SAP:** SLAM-associated protein · **Yaa:** Y chromosome-linked autoimmune acceleration

Full correspondence: Dr. Hiroyuki Nishimura, Toin Human Science and Technology Center, Department of Biomedical Engineering, Toin University of Yokohama, 1614 Kurogane-cho Aoba-ku, Yokohama 225-8502, Japan
Fax: +81-45-972-5972
e-mail: nisimura@cc.toin.ac.jp

Additional correspondence: Prof. Sachiko Hirose, Department of Pathology, Juntendo University School of Medicine, Tokyo, 113-8421, Japan
Fax: +81-3-3813-3164
e-mail: sacchi@juntendo.ac.jp

See accompanying Commentary:
http://dx.doi.org/10.1002/eji201141811

Received: 3/3/2011
Revised: 25/4/2011
Accepted: 20/5/2011
Accepted article online: 23/5/2011

Phenotype conversion from rheumatoid arthritis to systemic lupus erythematosus by introduction of *Yaa* mutation into FcγRIIB-deficient C57BL/6 mice

Shinya Kawano[*1], *Qingshun Lin*[*2], *Hirofumi Amano*[1], *Toshiyuki Kaneko*[1], *Keiko Nishikawa*[2], *Hiromichi Tsurui*[2], *Norihiro Tada*[3], *Hiroyuki Nishimura*[4], *Toshiyuki Takai*[5], *Toshikazu Shirai*[2], *Yoshinari Takasaki*[1] *and Sachiko Hirose*[2]

[1] Department of Internal Medicine, Juntendo University School of Medicine, Tokyo, Japan
[2] Department of Pathology, Juntendo University School of Medicine, Tokyo, Japan
[3] Atopy Research Center, Juntendo University School of Medicine, Tokyo, Japan
[4] Toin Human Science and Technology Center, Department of Biomedical Engineering, Toin University of Yokohama, Yokohama, Japan
[5] Department of Experimental Immunology and CREST of JST, Institute of Development, Aging and Cancer, Tohoku University, Sendai, Japan

We previously established an IgG Fc receptor IIB (FcγRIIB)-deficient C57BL/6 (B6)-congenic mouse strain (KO1), which spontaneously develops rheumatoid arthritis (RA), but not systemic lupus erythematosus (SLE). Here, we show that when Y chromosome-linked autoimmune acceleration (*Yaa*) mutation was introduced in KO1 strain (KO1.*Yaa*), the majority of KO1.*Yaa* mice did not develop RA, but instead did develop SLE. This phenotype conversion did not depend on autoantibody specificity, since KO1.*Yaa* mice, compared with KO1, showed a marked increase in serum levels of both lupus-related and RA-related autoantibodies. The increase in frequencies of CD69$^+$ activated B cells and T cells, and the spontaneous splenic GC formation with T follicular helper cell generation were manifest early in life of KO1.*Yaa*, but not KO1 and B6.*Yaa*, mice. Activated CD4$^+$ T cells from KO1.*Yaa* mice showed upregulated production of IL-21 and IL-10, compared with the finding in KO1 mice, indicating the possibility that this aberrant cytokine milieu relates to the disease phenotype conversion. Thus, our model is useful to clarify the shared and the disease-specific mechanisms underlying the clinically distinct systemic autoimmune diseases RA and SLE.

Keywords: Cytokines · FcγRIIB receptor · Rheumatoid arthritis · Systemic lupus erythematosus · *Yaa* mutation

Introduction

IgG Fc receptor IIB (FcγRIIB) is a major negative regulator of BCR-mediated activation signals in B cells [1]. We previously found that the *Fcgr2b* gene encoding FcγRIIB is polymorphic, and that autoimmune disease-prone mouse strains, such as NZB, BXSB, MRL, and NOD, all share deletion polymorphism in the AP-4-binding site in the *Fcgr2b* promoter region [2]. Because of the

Correspondence: Prof. Sachiko Hirose
e-mail: sacchi@juntendo.ac.jp

*These authors contributed equally to this work.

defective AP-4 binding, mice with this autoimmune-type allele polymorphism show downregulation of FcγRIIB expression levels in activated GC B cells, resulting in upregulation of IgG autoantibody production [3, 4]. These observations suggested that the autoimmune-type *Fcgr2b* confers the basis of susceptibility to autoimmune diseases. Consistent was our earlier finding that systemic lupus erythematosus (SLE) phenotypes in BXSB male mice carrying Y chromosome-linked autoimmune acceleration (*Yaa*) mutation were almost completely inhibited by the substitution of the autoimmune-type *Fcgr2b* for the wild C57BL/6 (B6)-type *Fcgr2b* [5]. However, because BXSB female mice carrying the autoimmune-type *Fcgr2b* but lacking *Yaa* did not develop SLE, it is likely that the autoimmune-type *Fcgr2b* contributes to SLE susceptibility through a strong epistatic interaction with *Yaa* mutation.

To examine further the role of the downregulated expression of FcγRIIB in autoimmune diseases, we recently established an FcγRIIB-deficient B6 mouse strain, KO1, by gene targeting in 129-derived embrionic stem cells and selective backcrossing to a B6 background. Intriguingly, KO1 did not develop SLE, but instead developed severe rheumatoid arthritis (RA), as reported previously [6]. This KO1 strain carried a 129-derived approximately 6.3 Mb interval distal from the null-mutated *Fcgr2b* gene within the *Sle16* locus, which is shown to induce loss of self-tolerance in the B6 background [7]. Boross et al. [8] reported that FcγRIIB-deficient B6 mice generated by gene targeting in B6-derived embryonic stem cells, thus lacking the 129-derived flanking *Sle16* locus, fail to develop any sign of autoimmune diseases. Thus, the development of RA in KO1 mice may be due to the epistatic interaction of FcγRIIB deficiency and *Sle16* locus.

Boross et al. [8] also reported that their FcγRIIB-deficient B6 mice develop lethal lupus nephritis in the presence of *Yaa* mutation, indicating the epistatsis between FcγRIIB-deficiency and *Yaa* in the development of full-blown autoimmune diseases. In addition, Subramanian et al. [9] reported that the strong epistatic interaction between *Yaa* and *Sle1*, which contains the autoimmune-predisposing *Slam/Cd2* haplotype, contributes to severe lupus nephritis. The *Sle16* locus also contains this autoimmune-predisposing *Slam/Cd2* haplotype [10].

In contrast to the accelerated effect of *Yaa* on lupus nephritis, Jansson and Holmdahl [11] reported the suppressive effect of *Yaa* on collagen-induced arthritis. In the present study, we have introduced *Yaa* mutation into FcγRIIB-deficient RA-prone KO1 mice to examine how *Yaa* affects the disease phenotypes in these mice. We found that the majority of KO1.*Yaa* mice did not develop RA, but instead did develop severe SLE early in life, and that this phenotype conversion did not depend on the shift of autoantibody specificity from RA-related to lupus-related one.

Characteristic clinical features differ between RA and SLE; however, both diseases share aberrant activation of immune processes associated with the production of a variety of autoantibodies and subsequent immune complex-mediated tissue inflammation. Our model is useful to investigate the shared and the disease-specific factors contributing to the clinically distinct systemic autoimmune diseases RA and SLE.

Results

Disease phenotype in Yaa-carrying FcγRIIB-deficient KO1 mice

KO1 mice developed arthritis after 4 months of age and the disease incidence and severity were increased with age. At 8 months of age, 67% of KO1 mice showed arthritis with marked swelling and stiffness of forepaws and hindpaws. In contrast, the incidence and severity of arthritis were markedly suppressed in KO1.*Yaa* mice and 88% of KO1.*Yaa* mice were free from arthritis (Fig. 1A). Representative macroscopic findings of forepaws and hindpaws of KO1 and KO1.*Yaa* mice at 8 months of age are shown in Figure 1B. Intriguingly, KO1 strain did not develop proteinuria; however, KO1.*Yaa* began to be positive for proteinuria at 2 months of age and the incidence of positive proteinuria reached 63% (Fig. 1C) with 46% mortality rate at 8 months of age (Fig. 1D).

Figure 1E shows a comparison of representative histopathological and immunofluorescent findings of renal glomeruli among B6, B6.*Yaa*, KO1, and KO1.*Yaa* mice at 4 months of age. In KO1.*Yaa* mice, glomeruli were significantly enlarged even at 4 months of age (Fig. 1F), because of a marked cellular proliferation in glomeruli and a large amount of IgG deposition in mesangial area and along glomerular capillary walls. These glomerular lesions were seldom observed in B6, B6.*Yaa*, and KO1 mice even at 8 months of age.

Serum levels of autoantibodies

To examine the relationship between the disease phenotype conversion from RA to SLE and the specificity of autoantibodies, we compared serum levels of lupus-related autoantibodies against dsDNA, chromatin, and RNP, and RA-related rheumatoid factor (RF), anti-type II collagen (CII), and -cyclic citrullinated peptide (CCP) antibodies at 2 and 6 months of age among B6, B6.*Yaa*, KO1, and KO1.*Yaa* mice (Fig. 2). KO1.*Yaa* mice showed higher serum levels of both lupus-related and RA-related autoantibodies than the other three strains of mice even at 2 months of age. The levels of all these antibodies were increased with age in KO1.*Yaa* mice. Age-associated increase was also observed in KO1 mice; however, the levels were remarkably higher in KO1.*Yaa* mice than those in KO1 mice at 6 months of age. Thus, the conversion of disease phenotype from RA to SLE was not explained by the shift of antibody specificity from RA-type to lupus-type.

Splenomegaly, subpopulation, and maturation/activation status of splenic lymphocytes

The spleen weight in B6, B6.*Yaa*, KO1, and KO1.*Yaa* mice was compared at 4 months of age. Splenomegaly was only observed in KO1.*Yaa* mice (Fig. 3A). Consistently, spontaneous GC formation was observed only in KO1.*Yaa* mice at 4 months of age (Fig. 3B).

Flow cytometric analysis of spleen cells from 4-month-old mice revealed that, while there were no differences in

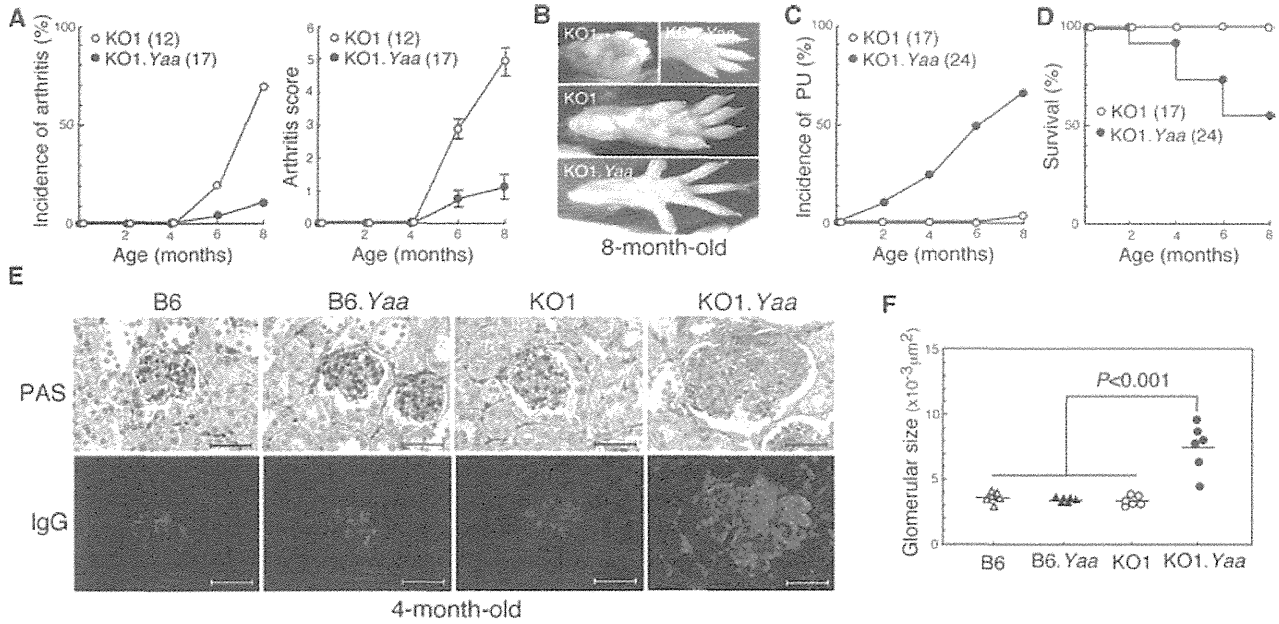

Figure 1. Disease phenotype shift from RA to SLE in KO1.*Yaa* mice. (A) Comparison of the cumulative incidence and score of arthritis between KO1 and KO1.*Yaa* mice. Score is shown as mean ± SE. (B) Representative macroscopic findings of forepaws and hindpaws in KO1 and KO1.*Yaa* mice at 8 months of age. The former mice show marked swelling and stiffness of the wrist and ankle joints. (C) Comparison of the cumulative incidence of proteinuria (PU) between KO1 and KO1.*Yaa* mice. (D) Comparison of survival rate between KO1 and KO1.*Yaa* mice. (E) Histopathological findings of glomeruli in B6, B6.*Yaa*, KO1, and KO1.*Yaa* at 4 months of age. Formalin-fixed sections were stained with periodic acid-Schiff/hematoxylin (PAS) (top). Frozen sections were stained with anti-mouse IgG (bottom) to evaluate the deposition of IgG in renal glomeruli. Scale bars = 50 μm. Representative results obtained from six mice in each strain. (F) Comparison of glomerular size as an indicator of the severity of glomerular lesion. The horizontal bar represents the mean. (A–F) All data are shown as the mean of the indicate numbers of mice in each panel and are representative of three experiments performed. Statistical significance was determined by Mann–Whitney's *U* test.

frequencies of $B220^+$ B cells per total spleen cells among four strains of mice (Table 1), there was a significant decrease in frequencies of $CD21^+CD23^-$ marginal zone B cells in *Yaa*-bearing B6.*Yaa* and KO1.*Yaa* mice (Fig. 4A and Table 1). This decrease is thought to be due to the effect of *Yaa* mutation, as reported previously [12], and not directly related to SLE phenotype. As for the activation/maturation status of B cells, frequencies of $CD69^+$ activated B cells, peanut agglutinin $(PNA)^+$ GC B cells, and $CD138^+$ plasma cells were significantly higher in KO1.*Yaa* mice than those found in other strains of mice (Fig. 4B and Table 1). As for T cells, while total $CD3^+$ T cells per total cells was significantly decreased in KO1.*Yaa* mice, the frequency of $CD69^+$ activated

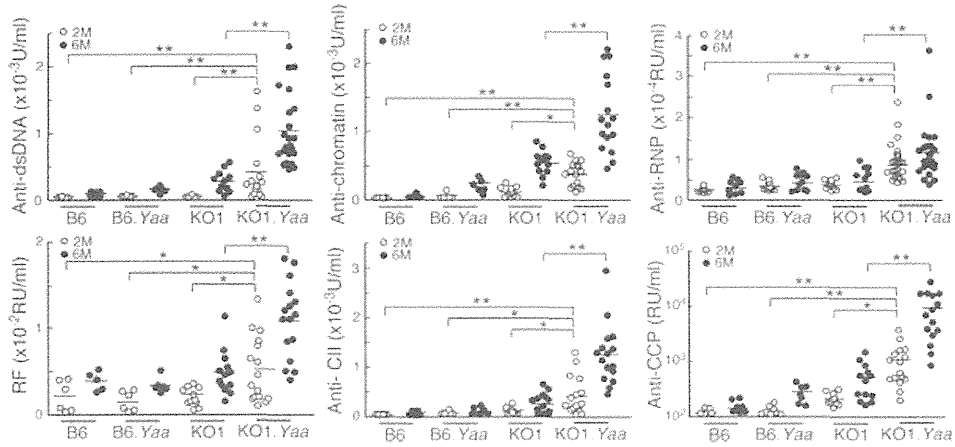

Figure 2. Comparisons of serum levels of lupus-related IgG autoantibodies against dsDNA, chromatin, and RNP, and RA-related IgG RF, anti-CII and -CCP antibodies among B6, B6.*Yaa*, KO1, and KO1.*Yaa* mice at 2 and 6 months of age. Each symbol represents an individual mouse and the bar represents the mean. Data shown are representative of three experiments performed. Statistical significance was determined by Mann–Whitney's *U* test (**$p < 0.001$, *$p < 0.05$).

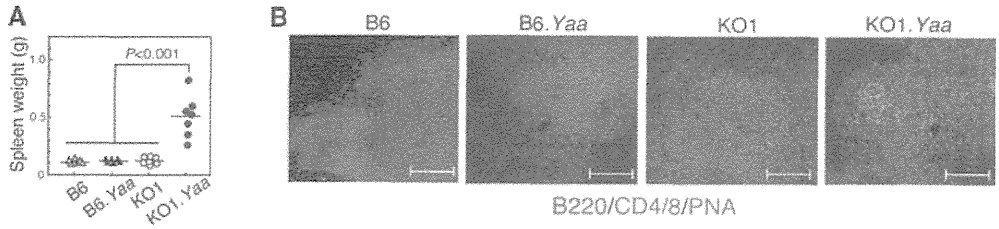

Figure 3. Splenomegaly with spontaneous GC formation in KO1.*Yaa* mice. (A) Comparison of spleen weight among B6, B6.*Yaa*, KO1, and KO1.*Yaa* mice at 4 months of age. Each symbol represents a single mouse and the bar represents the mean. Data shown are representative of three experiments performed. Statistical significance was determined by Mann–Whitney's *U* test. (B) Frozen spleen sections of 4-month-old mice were triple stained with a mixture of anti-CD4 and anti-CD8 mAbs (green), anti-B220 mAb (blue), and PNA (red) to examine the extent of GC formation. Representative results obtained from six mice in each strain are shown. Scale bar = 100 μm.

T cells was markedly increased in KO1.*Yaa* mice (Fig. 4C and Table 1). This activation of T cells may reflect the increases in the $CD4^+/CD8^+$ T-cell ratio and in the frequency of T_{FH} cells with $PD1^+ICOS^+CXCR5^+CD4^+$ phenotype (Fig. 4C and Table 1). Because the frequencies of $PD1^+ICOS^+CXCR5^+CD4^+$ T_{FH} cells in B6, B6.*Yaa*, and KO1 mice were within normal range (Table 1), the observed abnormal increase in $PD1^+ICOS^+CXCR5^+CD4^+$ T_{FH} cells in KO1.*Yaa* mice with overt SLE was thought to be due to the combined effect of the FcγRIIB-deficiency, *Sle16* locus, and *Yaa* mutation. Table 1 also shows that the frequency of $CD11b^+$ monocyte/macrophage population was significantly increased in KO1.*Yaa* mice with a comparable level observed in BXSB male mice [5].

Cytokine profile in spleen from KO1 and KO1.*Yaa* mice

To examine the difference in in vivo cytokine expression levels associated with phenotype conversion from RA to SLE, quantitative real-time PCR (qRT-PCR) analysis was performed to compare mRNA expression levels of notable cytokines in spleen between KO1 and KO1.*Yaa* mice at 4 months of age (Fig. 5A). The result showed that the expression of IL-6, IL-10, and IL-21 was significantly upregulated in KO1.*Yaa* mice compared with that in KO1 mice. Among these, the increase in IL-10 expression was prominent, with more than tenfold increase in KO1.*Yaa* mice. There was no significant difference in expression levels of other cytokines such as IL-2, IL-4, IL-17, IFN-γ, TNF-α, and IFN-α between two strains of mice.

We next examined the cellular source of IL-10 and IL-21, using flow cytometric analysis of PMA/ionomycin-stimulated spleen cells from 4-month-old KO1 and KO1.*Yaa* mice. Both IL-10 and IL-21 were secreted from $CD4^+$ T cells and the frequencies of IL-10 and IL-21-secreting cells per total $CD4^+$ T cells were significantly higher in KO1.*Yaa* than those in KO1 mice (mean ± SE of KO1 versus KO1.*Yaa*; IL-10: 7.56 ± 1.25 versus 14.74 ± 0.43, $p < 0.01$, IL-21: 5.09 ± 0.22 versus 9.91 ± 0.60, $p < 0.01$) (Fig. 5B), consistent with the results of qRT-PCR analysis. PD1 and ICOS expression levels were upregulated in in vitro stimulated $CD4^+$ T cells. Most IL-10 and IL-21-secreting cells showed high PD1 expression levels; however, the ICOS expression level was broadly distributed in these cytokine-secreting cells (Fig. 5B). As shown in Figure 5C, in addition to IL-10 and IL-21 single producers, the significant frequency of $CD4^+$ T cells secreted both cytokines.

Table 1. Subpopulations of splenocytes in KO1, KO1.*Yaa*, B6, and B6.*Yaa* mice at 4 months of age[a)]

	B6	B6.*Yaa*	KO1	KO1.*Yaa*
$B220^+$ B/total cells	50.5 ± 3.3	54.6 ± 3.4	53.5 ± 3.2	41.2 ± 5.7
$CD21^+CD23^-$ MZ B/total B	9.8 ± 0.8	2.7 ± 0.3[b)]	11.3 ± 1.2	2.3 ± 0.4[b)]
$CD69^+B220^+$ B/total B	2.7 ± 0.7	6.1 ± 1.8	2.3 ± 0.7	15.4 ± 2.8[c)]
PNA^+B220^+ B/total B	2.4 ± 0.2	2.4 ± 0.6	1.2 ± 0.1	8.1 ± 0.8[c)]
$CD138^+$ plasma/total cells	0.5 ± 0.0	1.0 ± 0.5	0.4 ± 0.1	2.6 ± 0.7[c)]
$CD3^+$ T/total cells	32.2 ± 1.6	27.9 ± 1.5	28.3 ± 2.1	18.8 ± 1.6[c)]
$CD69^+CD4^+$ T/total T	14.3 ± 2.1	19.3 ± 2.2	14.1 ± 1.3	44.6 ± 3.9[c)]
$CD4^+/CD8^+$ ratio	1.4 ± 0.1	1.6 ± 0.2	1.1 ± 0.1	6.1 ± 2.4[c)]
$CD25^+FoxP3^+CD4^+$ T/total T	18.0 ± 1.3	17.0 ± 1.3	16.0 ± 1.1	18.2 ± 0.2
$PD1^+ICOS^+CD4^+$ T/total T	2.6 ± 0.7	3.7 ± 1.2	2.1 ± 0.7	32.3 ± 3.4[c)]
$CXCR5^+PD1^+CD4^+$ T/total T	3.4 ± 0.8	3.7 ± 1.3	2.1 ± 0.7	13.2 ± 3.2[c)]
$CD11b^+$ cells/total cells	4.4 ± 0.5	4.7 ± 0.1	5.1 ± 0.2	13.3 ± 0.1[c)]

[a)] Results were obtained from six mice in each strain, and are shown as mean and SE.
[b)] The value is significantly different from B6 mice or KO1 mice ($p < 0.005$, Student's *t*-test).
[c)] The value is significantly different from other strains of mice ($p < 0.05$, Student's *t*-test).

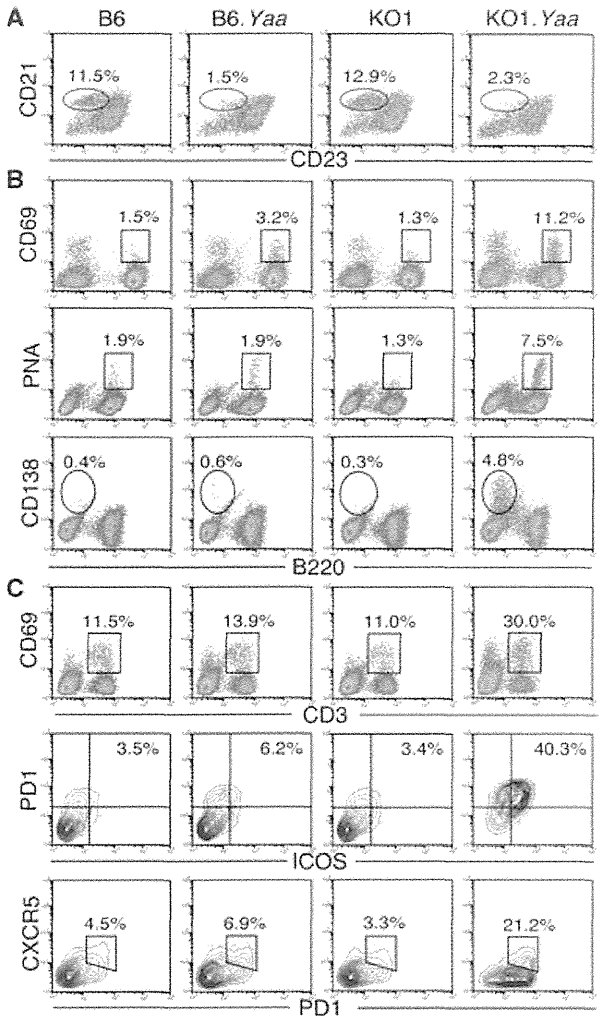

Figure 4. Comparisons of cell surface phenotypes of splenic lymphocytes among B6, B6.*Yaa*, KO1, and KO1.*Yaa* mice at 4 months of age, using flow cytometry. (A) Spleen cells were triple-stained with anti-B220, -CD21, and -CD23 mAbs, and CD21 and CD23 expression levels on $B220^+$ B cells were examined. The frequency of $CD21^+CD23^-$ marginal zone (MZ) B cells is shown. (B) Activation/maturation status of B cells. Spleen cells were stained with anti-CD69, -CD138, -B220 mAbs, and PNA. Frequencies of $CD69^+$ activated B cells per total B cells, PNA^+ GC B cells per total B cells, and $CD138^+$ plasma cells per total cells are shown. (C) Activation/maturation status of T cells. Spleen cells were stained with anti-CD69 and -CD3 mAbs, and the frequency of $CD69^+$ activated T cells per total $CD3^+$ T cells is shown. Cells were further stained with anti-CD4, -PD1, -ICOS, and -CXCR5 mAbs, and the frequencies of $PD1^+ICOS^+CD4^+$ and $PD1^+CXCR5^+CD4^+$ T_{FH} cells per total $CD4^+$ T cells are shown. Representative results obtained from six mice in each strain are shown.

Discussion

The current study showed that introduction of *Yaa* mutation into RA-prone KO1 mice leads to conversion of disease phenotypes from RA to SLE. RA and SLE are both classified as systemic autoimmune diseases. Since features of RA are occasionally associated with the clinical pictures of SLE [13], it has long been suggested that certain shared genetic pathways, as well as disease-specific ones, underlie the pathogenesis of both RA and SLE [14]. Our current model provided a clue to investigate this issue and suggested that, while the FcγRIIB deficiency and *Sle16* locus in KO1 genetic background confers predisposition to RA [6], an additional epistatic effect of *Yaa* mutation induces conversion of the disease phenotype from RA to SLE.

It has been shown that an etiology of *Yaa*-mediated B-cell activation is the duplication of the *Tlr7* gene [9,15,16]. The ligand for TLR7 is single-stranded RNA, thus suggesting that overexpression of TLR7 activates B cells by RNA-containing autoantigens, resulting in RNA-associated lupus autoantibody production. However, in the present study, *Yaa*-mediated disease phenotype conversion from RA to SLE was not explained by the shift of autoantibody specificity, and rather *Yaa*-mediated B-cell activation seems to be polyclonal in KO1.*Yaa* mice. This polyclonal B-cell activation may relate to the marked spontaneous GC formation and the T_{FH}-cell generation that developed in the spleen early in life of KO1.*Yaa* mice. The formation of GC depends on intrafollicular localization of antigen, activated B cells and T cells [17,18]. Among subsets of $CD4^+$ T cells, T_{FH} cells are the specialized subset to help B cells to generate affinity-matured antibodies [17]. In addition to the B-cell help by T_{FH} cells in GC reaction, it has been shown that the relationship between B cells and T_{FH} cells is a reciprocal dependency, and that the cognate interaction with activated B cells is required for the maintenance of $PD\text{-}1^+ICOS^+CXCR5^+$ T_{FH} cells [19]. This is consistent with the present study, in which the combined effect of FcγRIIB-deficiency, *Sle16* locus, and *Yaa* mutation accelerated not only spontaneous PNA^+ B-cell generation and GC formation but also T_{FH}-cell generation in KO1.*Yaa* mice. As this vicious cycle of activated B cells and T_{FH} cells promotes polyclonal B-cell activation, KO1.*Yaa* mice showed the marked increase in serum levels of both lupus-related and RA-related autoantibodies.

Anti-CCP antibodies are currently considered to be the most specific autoantibodies for RA patients, although some patients with SLE and Sjögren's syndrome were found to have these autoantibodies [20]. Anti-CCP antibodies react with citrullinated proteins, which are the product of posttranslational modification. Citrullination of protein is a physiological process and is catalyzed by peptidyl arginine deiminase enzymes. Anti-CCP antibodies may thus gain the arthritogenicity when citrullinated proteins are increased, particularly in the arthritic region [20]. In mouse models, an increased serum level of anti-CCP antibodies was observed in SLE-prone and arthritis-free *bcl-2*-transgenic (NZW × B6)F1 mice [21], as in the case of KO1.*Yaa* mice in the current study. Thus, it appears that this autoantibody specificity is not exclusively associated with inflammatory joint diseases.

In KO1.*Yaa* mice, there was a significant increase in the IL-21 expression level early in life compared with that in KO1 mice. IL-21 is a potent immunoregulatory cytokine produced by NKT cells and $CD4^+$ T cells, and it has recently been shown that IL-21 is an autocrine growth factor for T_{FH} cells [17,22]. Many cell types express the receptors for IL-21, but the level of expression on B cells is the highest and drives terminal differentiation of B cells and plasma cells [19,22]. Intriguingly, Bubier et al. [23]

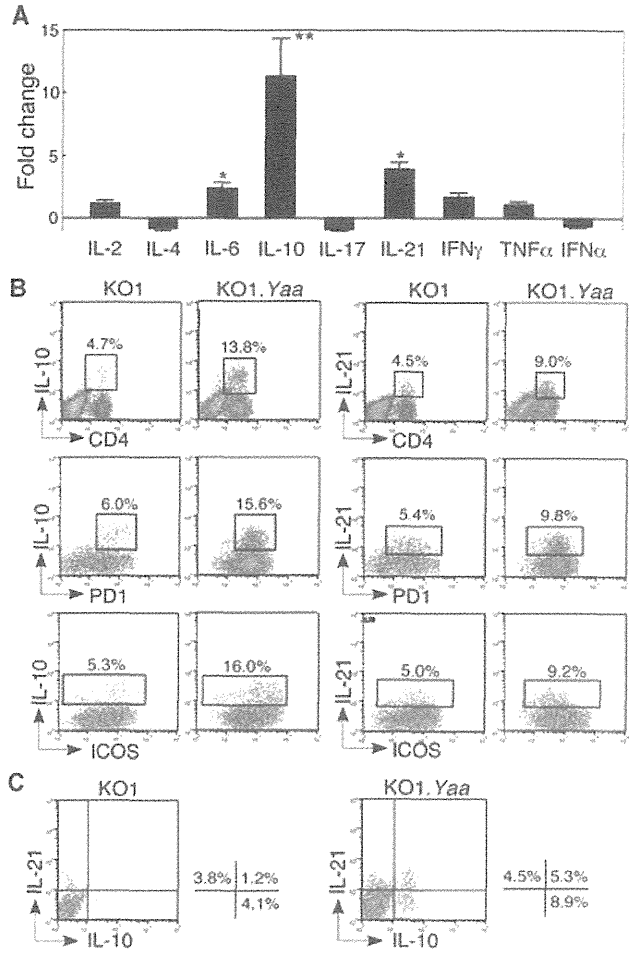

Figure 5. Comparisons of cytokine synthesis between KO1 and KO1.*Yaa* mice at 4 months of age. (A) Quantitative real-time PCR analysis of cytokine mRNA expression levels in spleen from KO1 and KO1.*Yaa* mice. Value of KO1 mice was designated as 1, and values of KO1.*Yaa* mice were evaluated as fold change compared with the values in KO1 mice. Data are shown as mean + SE of four mice for each strain and representative of three experiments performed. Statistical significance was determined by Mann–Whitney's *U* (*$p < 0.05$, **$p < 0.01$). (B) Flow cytometric analysis of IL-10 and IL-21-secreting cells in PMA/ionomycin-stimulated spleen cells from KO1 and KO1.*Yaa* mice. Frequencies of each cytokine secreting cells per total $CD4^+$ T cells, $CD4^+PD1^+$ T cells and $CD4^+ICOS^+$ T cells are shown. (C) Flow cytometric analysis of IL-10 and L-21-secreting cells, using gated $CD4^+$ T cells. Representative results obtained from six mice in each strain are shown.

reported that SLE phenotypes including autoantibody production in BXSB male mice were almost completely inhibited in the mice with the deficient IL-21 receptor. Furthermore, Rankin et al. [24] recently reported that IL-21 receptor-deficient MRL/*lpr* mice were devoid of abnormal systemic accumulation of activated B cells and T cells. These findings suggest that IL-21-mediated signals play an essential role for the pathogeneses of SLE.

It has been shown that IL-21 is a potent regulator of IL-10, since IL-10 production decreases in IL-21 receptor knockout mice, while it increases in IL-21-transgenic mice [25]. IL-10 was first described as a factor produced by Th2 cells, which inhibited the production of cytokines by Th1 cells [26]. Accumulating evidence, however, have shown that IL-10 is actually produced by many types of cells, and that, although IL-10 shows antiinflammatory properties against T cells and macrophages through inhibiting the production of inflammatory cytokines, it promotes B-cell function to induce antibody production [27, 28]. Considering these dual effects with immunosuppressive and immunostimulatory properties, IL-10 may confer different effects on the disease progression processes of RA and SLE. Indeed, the hallmark of RA is the excess production of inflammatory cytokines by T cells and macrophages at inflammatory foci, while SLE is characterized by increased production of high-affinity autoantibodies and deposition of their immune complexes in a wide variety of tissues, particularly in renal glomeruli. Consistently, there are several reports indicating the suppressive effect of IL-10 on RA [27, 29] and the promoting effect of IL-10 on lupus pathogenesis [30]. Further studies are needed to define the role of IL-10 in the conversion of disease phenotypes observed in the present study. These studies are underway in our laboratory.

Peripheral blood mononuclear cells from patients with active SLE show up-regulated expression of a group of type I IFN-induced genes [31–33]. Thus, IFN-α seems to be an important cytokine in SLE pathogenesis. In pristane-induced lupus model, the disease was shown to be associated with excess IFN-α production [34], as in the case of human SLE. However, overexpression of IFN-α is not likely to be involved in SLE pathogenesis in KO1.*Yaa* mice, since there were no differences in IFN-α expression levels between RA-prone KO1 mice and SLE-prone KO1.*Yaa* mice. Accumulating evidence shows that IL-6, IL-17, and TNF-α are important contributing cytokines to the pathogenesis of RA [35–37]. In the present studies, however, IL-6 expression levels were increased in SLE-prone KO1.*Yaa* mice compared with those in RA-prone KO1 mice, and there was no significant difference in expression levels of IL-17 and TNF-α between KO1 and KO1.*Yaa* mice. Thus, these cytokines are suggested to be unrelated to the observed phenotype conversion from RA to SLE in our model.

In conclusion, we introduced *Yaa* mutation into RA-prone KO1 strain and found that the disease phenotype converted from RA to SLE in KO1.*Yaa* mice. This phenotype conversion was likely to be due to the changes in cytokine milieus rather than the shift of autoantibody specificity from RA-related to lupus-related one. Further studies for the clarification and identification of the mechanism underlying this phenotype conversion are of paramount importance for shedding light on the mechanisms that control the development of clinically distinct systemic autoimmune diseases RA and SLE.

Materials and methods

Mice

FcγRIIB-deficient KO1 mice were generated by gene targeting in 129-derived embryonic stem cells and by backcrossing to B6 for over 12 generations [6]. The *Yaa* mutation was introduced into

KO1 mice by crossing with B6.*Yaa* mice. B6.*Yaa* mice were purchased from the Jackson Laboratory. All mice were housed under identical conditions. Experiments were performed in accordance with our institutional guidelines. Male mice were analyzed in the current study.

Incidence of arthritis

Ankle joint swelling was examined by inspection and arbitrarily scored as follows: 0, no swelling; 1, mild swelling; 2, moderated swelling; 3, severe swelling. Scores of both ankle joints are put together, and mice with scores over 2 were considered positive for arthritis.

Measurement of proteinuria

The proteinuria was monitored by biweekly testing and scored as previously descrobed [38]. Briefly, urine samples (10 μL) spotted on filter paper were air dried, fixed in 70% ethanol and stained with bromophenol blue solution. A series of standard three-fold dilution of BSA were processed as the same way, and the degree of proteinuria was assessed by visually comparing the color intensity of urine spot with that of the spot of BSA standards. Scores are as follows; 0:<37 mg/100 mL 1:≧37 mg/100 mL, 2:≧74 mg/mL, 3:≧111 mg/100 mL, 4:≧333 mg/100 mL, 5:≧1000 mg/100 mL, and 6:≧3000 mg/100 mL. Mice with urinary protein levels of four or more in repeated tests were considered as positive for proteinuria.

Histopathology and tissue immunofluorescence

Tissues fixed in 4% paraformaldehyde and embedded in paraffin were sectioned at 2 μm thickness, and tissue sections were stained with periodic acid-Schiff and hematoxylin (PAS). For immunofluorescence, tissues were embedded in Tissue-Tek OCT compound, frozen in liquid nitrogen, and sectined at 4 μm thickness. Frozen kidney sections were stained with FITC-labeled polyclonal goat anti-mouse IgG for 60 min at room temperature. For analysis of splenic tissues, frozen sections were three-color stained with Alexa 488-labeled anti-CD4 and -CD8 mAbs, Alexa 647-labeled anti-B220 mAb, and Alexa 546-labeled PNA. Antibodies and PNA were purchased from BD Pharmingen (San Diego, CA) and Vector Laboratories Inc. (Burlingame, CA), respectively. The labeling of these reagents was performed in our laboratory. Color images were obtained using laser scanning microscopy (Zeiss LSM510, Carl Zeiss Co., Ltd., Germany).

Estimation of the severity of glomerular lesion

The extent of cellular proliferation in glomerular lesion was estimated by the measurement of glomerular size. Kidney section stained by PAS was photographed under a microscope (Biozero, KEYENCE, Osaka, Japan) with ×50 magnification. Ten glomeruli in each field were randomly selected in order of size, and the size of each glomerulus was calculated using BZ-II analyzer software (KEYENCE). Mean size of 10 glomeruli was used as an indicator of histological severity of lupus nephritis in each individual mouse.

Serum levels of autoantibodies

Serum levels of IgG anti-dsDNA and -chromatin antibodies were measured using ELISA, as previously described [39]. Serum antibody levels are expressed in units, referring to a standard curve obtained by the serial dilution of a pooled serum of (NZB × NZW) F1 mice over 8 months, containing 1000 units/mL. Serum levels of IgG anti-RNP antibodies were measured by employing a commercially available kit (Alpha Diagnostic Intl. Inc., San Antonio, TX), and are expressed as relative units according to the manufacturer's instructions.

Serum levels of IgG RF and IgG anti-CCP antibodies were measured employing commercially available kits (Shibayagi Co. Ltd., Gunma, Japan and Cosmic Corporation, Tokyo, Japan, respectively), and are expressed as relative units according to the manufacturer's instructions. Serum levels of IgG anti-CII antibodies were measured using an ELISA plate precoated with bovine CII (Sigma-Aldrich, St. Louis, MO). CII-binding activities are expressed in units, referring to a standard curve obtained by serial dilution of a standard serum pool from KO1 mice hyper-immunized with CII, containing 1000 unit activities/mL.

Flow cytometric analysis

For the analysis of splenic lymphocytes, spleen cells were stained with the following reagents: FITC-conjugated anti-CD3, -CD21, -ICOS, -Foxp3, and -CD11b mAbs, Pacific blue-conjugated anti-B220, -CD4 mAbs, and PNA, PE-conjugated anti-B220, -CD138, -PD1, and -CD25 mAbs, and biotin-conjugated anti-CD69, -CD23, -CD8, and -CXCR5 mAbs, followed by streptavidin allophycocyanin. mAbs for CD25 and those for Foxp3, PD1, and ICOS were obtained from BioLegend (San Diego, CA) and eBioscience (San Diego, CA), respectively. Others were from BD PharMingen. Stained cells were four-color analyzed using a FACSAria cytometer and FlowJo software (Tree Star, Inc., Ashland, OR) with whole cell-gate excluding dead cells in forward and side scatter cytogram.

For intracellular cytokine staining of spleen cells, cells were stimulated with PMA (0.2 μg/mL)/ionomycin (2 μg/mL) in the presence of Golgi-Stop (BD Bioscience, San Jose, CA) for 5 h and stained with Pacific Blue-labeled anti-CD4 and biotin-labeled anti-PD1 or anti-ICOS mAbs followed by streptavidine allophycocyanin. Stained cells were then fixed and permeabilized using BD Cytofix/Cytoperm (BD Bioscience), followed by staining with FITC-labeled anti-IL-10, and PE-labeled anti-IL-21 mAbs. Stained cells were analyzed as above.

qRT-PCR analysis

Total RNA was isolated from spleen and first-stranded cDNA was synthesized using an oligo(dT)-primer with Superscript II First-Strand Synthesis kit (Invitrogen, Carlsbad, CA). The cDNA product was used for each qRT-PCR sample. The data were normalized to β-actin reference. Primer pairs used were as follows: IL-2 (forward) 5′-AACCTGAAACTCCCCAGGAT-3′, (reverse) 5′-AGGGCTT GTTGAGATGATGC-3′; IL-4 (forward) 5′-CCTCACAGCAACGAA GAACA-3′, (reverse) 5′-AAGTTAAAGCATGGTGGCTCA-3′; IL-6 (forward) 5′-GACAAAGCCAGAGTCCTTCAGAGAG-3′, (reverse) 5′-CTAGGTTTGCCGAGTAGATCTC-3′; IL-10 (forward) 5′-CCAA GCCTTATCGGAAATGA-3′, (reverse) 5′-TGGCCTTGTAGACACCT TGG-3′; IL-17 (forward) 5′-TCTCTGATGCTGTTGCTGCT-3′, (reverse) 5′-GACCAGGATCTCTTGCTGGA-3′; IL-21 (forward) 5′-ATCCTGAACTTCTATCAGCTCCAC-3′, (reverse) 5′-GCATTTAGCT ATGTGCTTCTGTTTC-3′; IFNγ (forward) 5′-AAGACAATCAGGCC ATCAGC-3′, (reverse) 5′-ATCAGCAGCGACTCCTTTTC-3′; TNF-α (forward) 5′-GGCAGGTCTACTTTGGAGTCATTGC-3′, (reverse) 5′-ACATTCGAGGCTGCTCCAGTGAATTCGG-3′; consensus IFNα (forward) 5′-ATGGCTAGRCTCTGTGCTTTCCT-3′, (reverse) 5′-AG GGCTCTCCAGAYTTCTGCTCTG-3′; β-actin (forward) 5′-AGCCAT GTACGTAGCCATCC-3′, and (reverse) 5′-CTCTCAGCTGTGGTGG TGAA-3′. The quantity was normalized using the formula of the $2^{-\Delta\Delta CT}$ method.

Statistical analysis

Statistical analysis was performed using Mann–Whitney's *U* test for disease phenotypes and Student's *t*-test for flow cytometric analysis. A value of $p < 0.05$ was considered as statistically significant.

Acknowledgments: The authors thank Dr. A. Sato-Hayashizaki, Mr. N. Ishihara, Ms. K. Kojyo, Ms. N. Ohtsuji, and Ms. T. Ikegami for excellent technical assistance. This work was supported in part by Grants-in-Aid for Scientific Research (C) from the Ministry of Education, Science, Technology, Sports and Culture of Japan, and Grant for Research on Intractable Diseases from the Ministry of Health, Labour, and Welfare of Japan.

Conflict of interest: The authors declare no financial or commercial conflict of interest.

References

1 Ravetch, J. V. and Kinet, J.-P., Fc receptors. *Annu. Rev. Immunol.* 1991. 9: 457–492.

2 Jiang, Y., Hirose, S., Abe, M., Sanokawa-Akakura, R., Ohtsuji, M., Mi, X., Li, N. et al., Polymorphisms in IgG Fc receptor IIB regulatory regions associated with autoimmune susceptibility. *Immunogenetics* 2000. 51: 429–435.

3 Jiang, Y., Hirose, S., Sanokawa-Akakura, R., Abe, M., Mi, X., Li, N., Miura, Y. et al., Genetically determined aberrant down-regulation of FcgRIIB1 in germinal center B cells associated with hyper-IgG and IgG autoantibodies in murine systemic lupus erythematosus. *Int. Immunol.* 1999. 11: 1685–1691.

4 Xiu, Y., Nakamura, K., Abe, M., Li, N., Wen, X-S., Jiang, Y., Zhang, D. et al., Transcriptional regulation of *Fcgr2b* gene by polymorphic promoter region and its contribution to humoral immune responses. *J. Immunol.* 2002. 169: 4340–4346.

5 Lin, Q., Xiu, Y., Jiang, Y., Tsurui, H., Nakamura, K., Kodera, S., Ohtsuhi, M. et al., Genetic dissection of the effects of stimulatory and inhibitory IgG Fc receptors on murine lupus. *J. Immunol.* 2006. 177: 1646–1654.

6 Sato-Hayashizaki, A., Ohtsuji, M., Lin, Q., Hou, R., Ohtsuji, N., Nishikawa, K., Tsurui, H. et al., Presumptive role of 129 strain-derived *Sle16* locus for rheumatoid arthritis in a new mouse model with FcgRIIB-deficient C57BL/6 genetic background. *Arthritis Rheum.* 2011. 63: 2930–2938.

7 Carlucci, F., Cortes-Hernandez, J., Fossati-Jimack, L., Bygrave, A. E., walport, M. J., Vyse, T. J., Cook, H. T. et al., Genetic dissection of spontaneous autoimmunity driven by 129-derived chromosome 1 loci when expressed on C57BL/6 mice. *J. Immunol.* 2007. 178: 2352–2360.

8 Boross, P., Arandhara, V. L., Martin-Ramirez, J., Santiago-Rober, M-L., Carlucci, F., Flierman, R., van der Kass, J. et al., The inhibiting Fc receptor for IgG, FcgRIIB, is a modifier of autoimmune susceptibility. *J. Immunol.* 2011. 187: 1304–1313.

9 Subramanian, S., Tus, K., Li, Q. Z., Wang, A., Tian, X. H., Zhou, J., Liang, C. et al., A *Tlr7* translocation accelerates systemic autoimmunity in murine lupus. *Proc. Natl. Acad. Sci. USA* 2006. 103: 9970–9975.

10 Wandstrat, A. E., Nguyen, C., Limaye, N., Chan, A. Y., Subramanian, S., Tian, X.-H., Yim, Y.-S. et al., Association of extensive polymorphisms in the SLAM/CD20 gene cluster with murine lupus. *Immunity* 2004. 21: 769–780.

11 Jansson, L. and Holmdahl, R., The Y chromosome-linked "autoimmune accelerating" *Yaa* gene suppresses collagen-induced arthritis. *Eur. J. Immunol.* 1994. 24: 1213–1217.

12 Amano, H., Amano, E., Moll, T., Marinkovic, D., Ibnou-Zekri, N., Martinez-Soria, E., Semac, I. et al., The *Yaa* mutation promoting murine lupus causes defective development of marginal zone B cells. *J. Immunol.* 2003. 170: 2293–2301.

13 Panush, R. S., Edwards, N. L., Longley, S. and Webster, E., 'Rhupus' syndrome. *Arch. Intern. Med.* 1988, 148: 1633–1636.

14 Jawaheer, D., Seldin, M. F., Amos, C. I., Chen, W. V., Shigeta, R., Monteio, J., Kern, M. et al., A genomewide screen in multiplex rheumatoid arthritis families suggests genetic overlap with autoimmune diseases. *Am. J. Hum. Genet.* 2001. 68: 927–936.

15 Pisitkunm, P., Deane, J. A., Difilippantonio, M. J., Tarasenko, T., Satterthwaite, A. B. and Bolland, S., Autoreactive B cell responses to RNA-related antigens due to *TLR7* gene duplication. *Science* 2006. 312: 1669–1672.

16 Deane, J. A., Pisitkun, P., Barrett, R. S., Feigenbaum, L., Town, T., Ward, J. M., Flavell, R. A. et al., Control of Toll-like receptor 7 expression is essential to restrict autoimmunity and dendritic cell proliferation. *Immunity* 2007. 27: 801–810.

17 King, C., Tangye, S. G. and Mackay, C. R., T follicular helper (TFH) cells in normal and dysregulated immune responses. *Annu. Rev. Immunol.* 2008. 26: 741–766.

18 Vinuesa, C. G., Sanz, I. and Cook, M. C., Dysregulation of germinal centers in autoimmune disease. *Nat. Rev. Immunol.* 2009. **9**: 845–857.

19 King, C., A fine romance: T follicular helper cells and B cells. *Immunity* 2011. **34**: 827–829.

20 Uysal, H., Nandakumar, K. S., Kessel, C., Carlsen, S., Burkhardt, H. and Holmdahl, R., Antibodies to citrullinated proteins: molecular interactions and arthritogenicity. *Immunol. Rev.* 2010. **133**: 9–33.

21 López-Hoyos, M., Marquina, R., Tamayo, E., González-Rojas, J., Izui, S., Merino, R. and Merino, J., Defects in the regulation of B cell apoptosis are required for the production of citrullinated peptide autoantibodies in mice. *Arthritis Rheum.* 2003. **48**: 2353–2361.

22 Spolski, R. and Leonard, W. J., Interleukin-21: basic biology and implications for cancer and autoimmunity. *Annu. Rev. Immunol.* 2008. **26**: 57–79.

23 Bubier, J. A., Sproule, T. J., Foreman, O., Spolski, R., Shaffer, D. J., Morse, H. C. III, Leonard, W. J. et al., A critical role for IL-21 receptor signaling in the pathogenesis of systemic lupus erythematosus in BXSB-*Yaa* mice. *Proc. Natl. Acad. Sci. USA* 2009. **106**: 1518–1523.

24 Rankin, A. L., Guay, H., Herber, D., Bertino, S. A., Duzanski, T. A., Carrier, Y., Keegan, S. et al., IL-21 receptor is required for the systemic accumulation of activated B and T lymphocytes in MRL/MpJ-Fas$^{lpr/lpr}$/J mice. *J. Immunol.* 2012. **188**: 1656–1667.

25 Spolski, R., Kim, H.-R., Zhu, W., Levy, D. E. and Leonard, W. J., IL-21 mediates suppressive effects via its induction of IL-10. *J. Immunol.* 2009. **182**: 2859–2867.

26 Fiorentino, D. F., Bond, M. W. and Moamann, T. R., Two types of mouse T helper cell. IV. Th2 clones secrete a factor that inhibits cytokine production by Th1 clones. *J. Exp. Med.* 1989. **170**: 2081–2095.

27 Moore, K. W., de Waal Malefyt, R., Coffman, R. L. and O'Garra, A., Interleukin-10 and the interleukin-10 receptor. *Annu. Rev. Immunol.* 2001. **19**: 683–765.

28 O'Garra, A., Barret, F. J., Castro, A. G., Vicari, A. and Hawrylowicz, C., Strategies for use of IL-10 or its antagonists in human disease. *Immunol. Rev.* 2008. **223**: 114–131.

29 Hata, H., Sakaguchi, N., Yoshitomi, H., Iwakura, Y., Sekikawa, K., Azuma, Y., Kanai, C. et al., Distinct contribution of IL-6, TNF-a, IL-1, and IL-10 to T cell-mediated spontaneous autoimmune arthritis in mice. *J. Clin. Invest.* 2004. **114**: 582–588.

30 Ishida, H., Muchamuel, T., Sakaguchi, S., Andrade, S., Menon, S. and Howard, M., Continuous administration of anti-interleukin 10 antibodies delays onset of autoimmunity in NZB/W F1 mice. *J. Exp. Med.* 1994. **179**: 305–210.

31 Baechler, E. C., Batliwalla, F. M., Karypis, G., Gaffney, P. M., Ortmann, W. A., Espe, K. J., Shark, K. B. et al., Interferon-inducible gene expression signature in peripheral blood cells of patients with severe lupus. *Proc. Natl. Acad. Sci. USA* 2003. **100**: 2610–2615.

32 Bennett, L., Palucka, A. K., Arce, E., Cantrell, V., Borvak, J., Banchereau, J. and Pascual, V., Interferon and granulopoiesis signatures in systemic lupus erythematosus blood. *J. Exp. Med.* 2003. **197**: 711–723.

33 Kirou, K. A., Lee, C., George, S., Louca, K., Papagiannis, I. G., Peterson, M. G., Ly, N. et al., Coordinate overexpression of interferon-a-induced genes in systemic lupus erythematosus. *Arthritis Rheum.* 2004. **50**: 3958–3967.

34 Reeve, W. H., Lee, P. Y., Weinstein, J. S., Aatoh, M. and Lu, L., Induction of autoimmunity by pristine and other naturally occurring hydrocarbons. *Trends in Immunol.* 2009. **30**: 455–464.

35 Ishihara, K. and Hirano, T., IL-6 in autoimmune disease and chronic inflammatory proliferative disease. *Cytokine Growth Factor Rev.* 2002. **13**: 357–368.

36 Iwakura, Y., Nakae, S., Saijo, S. and Ishigame, H., The role of IL-17A in inflammatory immune responses and host defence against pathogens. *Immunol. Rev.* 2008. **226**: 57–79.

37 Banchereau, J., Pascual, V. and Palucka, A. K., Autoimmunity through cytokine-induced dendritic cell activation. *Immunity* 2004. **20**: 539–550.

38 Knight, J. G., Adams, D. D. and Purves, H. D., The genetic contribution of the NZB mouse to the renal disease of the NZB x NZW hybrid. *Clin. Exp. Immunol.* 1977. **28**: 352–358.

39 Zhang, D., Fujio, K., Jiang, Y., Zhao, J., Tada, N., Sudo, K., Tsurui, H. et al., Dissection of the role of MHC class II A and E genes in autoimmune susceptibility in murine lupus models with intragenic recombination. *Proc. Natl. Acad. Sci. USA* 2004. **101**: 13838–13843.

Abbreviations: **B6**: C57BL/6 mice · **CII**: type II collagen · **CCP**: cyclic citrullinated peptide · **FcγRIIB**: IgG Fc receptor IIB · **PNA**: peanut agglutinin · **RA**: rheumatoid arthritis · **RF**: rheumatic factor · **SLE**: systemic lupus erythematosus · **qRT-PCR**: quantitative real-time PCR · ***Yaa***: Y chromosome-linked autoimmune acceleration mutation

Full correspondence: Prof. Sachiko Hirose, Department of Pathology, Juntendo University School of Medicine, 2–1-1 Hongo, Bunkyo-ku, Tokyo 113-8421, Japan
Fax: +81-3-3813-3164
e-mail: sacchi@juntendo.ac.jp

Received: 10/10/2012
Revised: 28/11/2012
Accepted: 17/12/2012
Accepted article online: 26/12/2012

THE JOURNAL OF BIOLOGICAL CHEMISTRY VOL. 286, NO. 50, pp. 43465–43474, December 16, 2011

GRAIL (Gene Related to Anergy in Lymphocytes) Regulates Cytoskeletal Reorganization through Ubiquitination and Degradation of Arp2/3 Subunit 5 and Coronin 1A*[S]

Received for publication, January 19, 2011, and in revised form, October 5, 2011 Published, JBC Papers in Press, October 20, 2011, DOI 10.1074/jbc.M111.222711

Daiju Ichikawa, Miho Mizuno, Takashi Yamamura, and Sachiko Miyake[1]

From the Department of Immunology, National Institute of Neuroscience, National Center of Neurology and Psychiatry, 4-1-1 Ogawahigashi, Kodaira, Tokyo 187-8502, Japan

Anergy is an important mechanism for the maintenance of peripheral tolerance and avoidance of autoimmunity. The up-regulation of E3 ubiqitin ligases, including GRAIL (gene related to anergy in lymphocytes), is a key event in the induction and preservation of anergy in T cells. However, the mechanisms of GRAIL-mediated anergy induction are still not completely understood. We examined which proteins serve as substrates for GRAIL in anergic T cells. Arp2/3-5 (actin-related protein 2/3 subunit 5) and coronin 1A were polyubiquitinated by GRAIL via Lys-48 and Lys-63 linkages. In anergic T cells and GRAIL-overexpressed T cells, the expression of Arp2/3-5 and coronin 1A was reduced. Furthermore, we demonstrated that GRAIL impaired lamellipodium formation and reduced the accumulation of F-actin at the immunological synapse. GRAIL functions via the ubiquitination and degradation of actin cytoskeleton-associated proteins, in particular Arp2/3-5 and coronin 1A. These data reveal that GRAIL regulates proteins involved in the actin cytoskeletal organization, thereby maintaining the unresponsive state of anergic T cells.

The regulation of T cell activation ensures efficient elimination of pathogens, as well as the maintenance of tolerance to self. Peripheral tolerance prevents the expansion of self-reactive T cells that escaped thymic selection, thus avoiding autoimmunity. T cell anergy is one form of peripheral tolerance that results in nonresponsiveness to antigen rechallenge following an initial partial activation; partial initial activation may result from the stimulation of T cell receptor (TCR)[2] in the absence of co-stimulation or the stimulation of T cells with the calcium ionophore ionomycin (1, 2). The induction of T cell anergy is inhibited by the addition of cyclohexamide, suggesting that anergy induction requires new protein synthesis (3). Recent reports have demonstrated that the induction of E3 ubiquitin ligases, including CBL-b, Itch, Deltex-1, and GRAIL (gene related to anergy in lymphocytes), is required to induce and maintain T cell anergy (4–8). In particular, it is well known that Cbl and Cbl-b act as negative regulators of TCR or CD28 signal transduction cascade through their ability to ubiquitinate tyrosine kinases including Src family kinases such as Fyn and Lck; Syk family kinases such as ZAP-70, Syk, PKC-θ, phospholipase C-γ, and p85; and the regulatory subunit of PI3K (4, 5, 9–15).

GRAIL is a type I transmembrane E3 ligase identified as an early gene that promotes T cell anergy (8). The up-regulation of GRAIL was observed in anergic CD4 T cells after treatment with ionomycin *in vitro* (4). Overexpression of GRAIL in T cell hybridomas or in primary cells reduces IL-2 production as well as proliferation upon antigen stimulation. Naive T cells from *GRAIL*-deficient mice exhibit increased proliferation and cytokine expression upon activation compared with those from control mice and do not depend on co-stimulation for effector generation (16, 17). Moreover, *GRAIL*-deficient mice exhibit lymphocyte infiltration into the lung and kidney and exacerbation of experimental autoimmune encephalomyelitis, indicating an important role for GRAIL in preventing lymphoproliferative and autoimmune responses (17). Although several candidates for GRAIL targets have been reported, including membrane proteins such as CD40 ligand and cytosolic proteins such as Rho GDIs, the mechanisms of GRAIL-mediated anergy induction are still not completely understood (18–21).

T cell activation and function require a structured engagement of antigen-presenting cells. These cell contacts are characterized by prolonged contacts from stable junctions called immunological synapses (IS). Reorganization of the actin cytoskeleton plays an important role in IS formation and signaling. Treatment of T cells with the actin-destabilizing agent cytochalasin D inhibits TCR-mediated IL-2 gene transcription (22). The Arp2/3 (actin-related protein 2/3) complex has been reported to be essential for TCR-mediated cytoskeletal reorganization (23, 24), and Arp2/3 complex-mediated actin nucleation is required for the formation of an F-actin-rich lamellipod (22, 25, 26). Coronin 1A is preferentially expressed in hematopoietic cells and co-localizes with F-actin-rich membranes in activated T cells (27). Coronin 1A has been shown to bind the Arp2/3 complex and inhibit F-actin nucleation by freezing the Arp2/3 complex in its inactive conformation (28). *Coronin 1A*-deficient T cells exhibit reduced cytokine production, including of IL-2 and IFN-γ, and altered F-actin reorganization (29). Moreover, a nonsense mutation in coronin 1A was identified as a gene alteration associated with the Lmb3 locus, which

* This work was supported by Grant-in-Aid for Scientific Research B: 7210 (to S. M.) and Grant-in-Aid for Young Scientists B: 20790093 (to D. I.) from the Japan Society for the Promotion of Science, and Health and Labor Sciences Research Grants for Research on Intractable Diseases from the Ministry of Health, Labor and Welfare of Japan.

[S] The on-line version of this article (available at http://www.jbc.org) contains supplemental text, Table S1, and Figs. S1 and S2.

[1] To whom correspondence should be addressed: 4-1-1 Ogawahigashi, Kodaira, Tokyo 187-8502, Japan. Tel.: 81-423-41-2711; Fax: 81-42-346-1753; E-mail: miyake@ncnp.go.jp.

[2] The abbreviations used are: TCR, T cell receptor; IS, immunological synapse(s); OVA, ovalbumin; Ab, antibody; Ub, ubiquitin.

plays a major role in modulating autoimmunity in Fas^{lpr} mice (30).

In the present study, we demonstrate that both Arp2/3 subunit 5 (Arp2/3-5), a component of the Arp2/3 complex, and coronin 1A serve as substrates for GRAIL. The expression of Arp2/3-5 and coronin 1A is reduced in anergic T cells and in T cells in which GRAIL is overexpressed. Retroviral-driven expression of Arp2/3-5 or coronin 1A in anergic ovalbumin (OVA)-specific T cells restores their proliferation upon antigen activation. The accumulation of F-actin, Arp2/3-5, and coronin 1A at the IS is decreased in anergic T cells as well as in T cells overexpressing GRAIL. Thus, our findings demonstrate that GRAIL maintains the anergic states of T cells by regulating IS formation via degradation of the actin cytoskeleton-associated proteins Arp2/3-5 and coronin 1A.

EXPERIMENTAL PROCEDURES

Reagents and Antibodies—We obtained ionomycin, polybrene, and OVA from Sigma-Aldrich, OVA peptide ($OVA_{323-339}$) from TORAY Laboratory (Tokyo), lactacystin from Boston Biochem Inc., and recombinant IL-2 from Pepro Tech. We purchased antibodies (Abs) against Arp2/3-5 (C3), c-Myc (9E10), HA (F7), and GAPDH (6C5) from Santa Cruz Biotechnology, anti-Arp2/3-5 from Epitomics Inc. (Burlingame, CA), anti-coronin 1A from Everest Biotech Ltd. (Oxfordshire, UK), anti-CD28 Ab from BD Bioscience (San Jose, CA), and peroxidase-conjugated anti-rabbit IgG, anti-goat IgG, and anti-mouse IgG from DAKO-Japan (Tokyo). We obtained the pcDNA4-V5/His vector, pcDNA4-Myc/His vector, and SNARF-1 from Invitrogen and the pAcGFP1-N1 vector from Clontech Laboratories, Inc. HA-conjugated wild-type or mutated ubiquitin constructs were kind gifts from Dr. C. Akazawa at Tokyo Medical and Dental University. pAlter-MAX HA-Cbl-b was a kind gift from Dr. H. Band (University of Nebraska Medical Center).

Mice—DO11.10, OVA-specific TCR-transgenic mice were purchased from Jackson Laboratories. Seven-week-old female C57BL/6J mice were purchased from CLEA Laboratory Animal Corporation (Tokyo, Japan). The animals were maintained in specific pathogen-free conditions, and all care and use procedures were in accordance with institutional guidelines.

Cell Culture and Proliferation—DO11.10 splenocytes were cultured in complete DMEM (Invitrogen) supplemented with 0.05 mM 2-mercaptoethanol, 100 units/ml penicillin/streptomycin, and 10% FBS. Proliferative responses after 2 days of stimulation with plate-bound anti-CD3 (0.5 μg/ml) and anti-CD28 (1 μg/ml) Abs were determined by [^{3}H]thymidine incorporation using a β-1205 counter (Pharmacia). To induce anergy *in vitro*, DO11.10 splenocytes incubated with 1 mg/ml OVA for 3 days were rested for 7–10 days and were then stimulated for 18 h with ionomycin (1 μg/ml) (3).

Constructs—GRAIL, Arp2/3-5, coronin 1A, RhoGDIα, RhoGDIβ, Lasp1, and RGS10 cDNAs from DO11.10 T cells in which anergy had been induced by ionomycin were amplified with following the specific PCR primers: GRAIL, 5′-CAGTGAATTCATGGGGCCGCCGCCCGGGATC-3′ and 5′-CAGTCTCGAGAGATTTAATCTCCCGAACAGCAGC-3′; Arp2/3-5, 5′-CATGGAATTCTCCGGGATGTCGAAGAACACGGTGTC-3′ and 5′-GATCGCGGCCGCCACGGTTTTCCTTGCAGTCA-3′; coronin1A, 5′-GATCGCGGCCGCCTACTTGGCCTGAACAGTCT-3′ and 5′-CAGTCTCGAGCTTGGCCTGAACAGTCTCCTC-3′; RhoGDIα, 5′-CATGGAATTCGTAAGCATGGCAGAACAGGAACCCAC-3′ and 5′-GATCGCGGCCGCGTCCTTCCACTCCTTTTTGA-3′; RhoGDIβ, 5′-CATGGGATCCATCAAGATGACGGAGAAGGATGCACA-3′ and 5′-GATCGCGGCCGTTCTGTCCAATCCTTCTTAA-3′; and RGS10, 5′-CAGTGGATCCATGTTCACCCGCGCCGTG-3′ and 5′-CAGTCTCGAGTGTGTTGTAAATTCTGGAGGCTCG-3′. SOD1 cDNA from brain was amplified with the following PCR primers: 5′-CAGTGAATTCATGGCGATGAAAGCGGTGTGC-3′ and 5′-CAGTCTCGAGCTGCGCAATCCCAATCACTCC-3′. PCR products were cloned into a pcDNA4 V5/His vector or pcDNA4 Myc/His vector. The H297N and H300N mutations in the RING domain of murine GRAIL were generated using a PCR site-directed mutagenesis kit (Stratagene, Santa Clara, CA). Deletion of the RING domain in murine GRAIL was generated using the following PCR primers: for the 5′-PCR product, CAGTGAATTCATGGGGCCGCCGCCCGGGATC and CAGTTTCGAATCTCCATCAGGGCCAATTTC; and for the 3′-PCR product, CAGTTTCGAAGTGTGACATTCTCAAAGCT and CAGTCTCGAGAGATTTAATCTCCCGAACAGCAGC. After these reactions, the DNAs were digested with BamHI and HpaI, and the fragments, which were WT-GRAIL-V5/His, H2N2-GRAIL-V5/His, ΔRF-GRAIL-V5/His, Arp2/3-5-Myc/His, coronin 1A-Myc/His, RhoGDIα-Myc/His or RhoGDIβ-Myc/His, were subcloned into a pMIG vector. After pcDNA4 WT-GRAIL-V5/His was digested with NheI and XhoI, the fragment was subcloned into pAcGFP N1 vector.

Retroviral Transductions and Proliferation of Transfected T Cells—HEK293T cells were transfected with a pMIG plasmid and pCLEco helper plasmid by calcium phosphate precipitation. Supernatants were collected 48 and 72 h later and filtered through 0.45-μm syringe filters (Millipore, MA). Activated DO11.10 CD4$^+$T cells were resuspended in the collected supernatant (1×10^6 cells/ml) with recombinant IL-2 (50 units/ml) and polybrene (8 μg/ml) and were centrifuged at 2,500 rpm for 90 min. Transfected cells were expanded in complete DMEM with recombinant IL-2 for 48 h and were rested without IL-2. After treatment with ionomycin (0.3 μg/ml) for 18 h, the cells were stained with SNARF-1 (5 μM) for 15 min and were stimulated with plate-bound anti-CD3 and anti-CD28 Abs. Two days later, proliferation was analyzed using a FACSCalibur and the CELLQuest program (BD Biosciences).

Western Blot Analysis—The cells were washed with PBS and lysed in 1% Nonidet P-40 lysis buffer (137 mM NaCl, 1% Nonidet P-40, 10% glycerol, 20 mM Tris, pH 7.5). After incubation for 10 min on ice, lysates were centrifuged at 13,200 rpm for 15 min at 4 °C, and supernatants were collected. After adjustment of protein concentrations using the Dc protein assay (Bio-Rad), the lysates were mixed with Laemmli's buffer (1.33% SDS, 10% glycerol, 2% 2-mercaptoethanol, 0.002% bromphenol blue, 83 mM Tris, pH 6.8) and were boiled for 5 min. Lysates (10–30 μg) were subjected to 10 or 12% SDS-PAGE and immobilized on nitrocellulose membranes. The membranes were blocked with 5% milk, PBS, 0.05% Tween for 1 h at room temperature. Proteins were detected with various Abs (mostly diluted at 1:1000)

and horseradish peroxidase-coupled anti-rabbit, anti-mouse, or anti-goat IgG Abs (1:1000). The proteins were visualized using an enhanced chemiluminescence Western blot detection system (Amersham Biosciences).

Ubiquitination Assay—HEK293T cells were co-transfected with V5/His-tagged GRAIL, HA-tagged ubiquitin, and Myc/His-tagged substrate-containing expression vectors. Twenty-four hours later, the cells were incubated with 0.3 μM lactacystin for 12 h. The cells were lysed using 1% Nonidet P-40 lysis buffer containing protease inhibitors (Complete protease inhibitor mixture; Roche Applied Science) and were subjected to immunoprecipitation with anti-Myc Ab. Ubiquitination of substrates was analyzed by SDS-PAGE after blotting with anti-HA Ab.

Immunofluorescence Microscopy—To investigate co-localization of GRAIL and its substrates, HEK293T cells were co-transfected by calcium phosphate precipitation with the pAcGFP1-N1 vector containing GRAIL and pcDNA4-DsRed vector containing the substrate. Twenty-four hours later, the cells were incubated with lactacystin (0.3 μM) for 12 h and were fixed with MeOH for 15 min at 4 °C. To analyze T cell-B cell conjugation, A20 cells pulsed with 1 μg/ml $OVA_{323-339}$ for 2 h at 37 °C were incubated at a ratio of 1:1 with transfected GFP^+DO11.10 $CD4^+$T cells sorted on a FACS Aria cell sorter (BD Biosciences) at 37 °C for 10 min. The cells were then plated on poly-L-lysine-coated slides for 15 min. To analyze lamellipodium formation, T cells overexpressing the control or indicated constructs were settled onto anti-CD3-coated coverslips for 5 min as described previously (26). The cells were fixed with 4% paraformaldehyde for 15 min at 4 °C and washed with PBS, 0.01% Tween 20. After blocking with PBS, 1% BSA for 1 h at room temperature, the cells were incubated with either anti-Arp2/3-5 (C3) or anti-coronin 1A Ab for 18 h at 4 °C. After washing, the cells were labeled with Cy5-conjugated anti-mouse IgG or anti-goat IgG (Jackson ImmunoResearch Laboratories, West Grove, PA) for 2 h at room temperature. The slides were mounted with ProLong Gold antifade reagent (Invitrogen) with or without DAPI. Confocal images were acquired using FV1000-D (Olympus, Tokyo, Japan).

Statistical Analysis—Statistical differences between control and treatment groups were assessed with the Student's *t* test.

Additional Procedures—Information on semiquantitative RT-PCR and generation of shRNA is available in the supplemental materials.

RESULTS

Reduced Expression of Arp2/3-5 and Coronin 1A—E3 ubiquitin ligases including GRAIL are up-regulated in anergized T cells and play an important role in the induction of anergy (4, 8). To determine which proteins serve as substrates for GRAIL, we used two-dimensional difference gel electrophoresis to analyze proteins that were down-regulated in T cells in which anergy had been induced by ionomycin. Down-regulated proteins were identified by MALDI-TOF-MS and the nonredundant NCBI (NCBInr) database using MASCOT software (supplemental Table S1). Proteins related to cytoskeletal reorganization were the most frequently down-regulated proteins in anergic T cells. We decided to focus on actin-related proteins Arp2/3-5 and coronin 1A. We first confirmed that the expression levels of these proteins were reduced in T cells in ionomycin-induced anergy. We stimulated splenocytes of DO11.10 mice with OVA protein for 3 days and then rested them for 7 days. Anergy was induced by the addition of ionomycin for 18 h and the proliferative response upon the addition of anti-CD3 and anti-CD28 Abs detected by the incorporation of [^{3}H]thymidine. The proliferative response was significantly suppressed in ionomycin-treated cells, confirming that anergy was properly induced (Fig. 1*A*). In these anergized cells, the protein expression of Arp2/3-5 and coronin 1A was reduced (Fig. 1*B*, *lanes 2* and *4*). To address the functional involvement of Arp2/3-5 and coronin 1A in T cell anergy, we examined whether overexpression of these proteins in DO11.10 $CD4^+$ T cells enhanced their proliferative response upon stimulation. DO11.10 $CD4^+$ T cells were transfected with Arp2/3-5 or coronin 1A. To analyze proliferation of transfected T cells by flow cytometry, the cells were treated with ionomycin and labeled with SNARF-1, which can monitor proliferating cells through dye dilution in a similar fashion to CFSE dilution assay. The number of proliferating cells upon stimulation (GFP^+ $SNARF\text{-}1^-$ cells) was increased in Arp2/3-5 or coronin 1A-overexpressing cells compared with that of control cells (Fig. 1*C*). We also analyzed whether an anergy-like state was displayed by knockdown of Arp2/3-5 or coronin 1A. The percentage of proliferation increase upon the restimulation with anti-CD3/anti-CD28 was decreased in Arp2/3-5 shRNA-expressing T cells (8%) and in coronin 1A shRNA-expressing T cells (3%) compared with that in control shRNA-expressing cells (13%). These results indicate that the expression of Arp2/3-5 and coronin 1A is correlated with T cell responses and is reduced in anergic T cells.

GRAIL Polyubiquitinates Arp2/3-5 and Coronin 1A—We next examined whether Arp2/3-5 and coronin 1A serve as substrates for GRAIL. Myc-tagged Arp2/3-5, coronin 1A or other candidate substrate proteins were transiently co-expressed with V5-tagged GRAIL and HA-tagged ubiquitin (Ub) in HEK293T cells. Twenty-four hours after transfection, the cells were treated with the proteasome inhibitor lactacystin for 12 h, and then lysates were prepared and immunoprecipitated with an anti-Myc Ab. SDS-PAGE followed by immunoblotting with anti-HA revealed a polyubiquitinated laddering pattern of Arp2/3-5 and coronin 1A in the presence of GRAIL (Fig. 2*A*, *lanes 6* and *10*). As Rho GDP dissociation inhibitors (RhoGDI) α and β were previously reported as substrates of GRAIL, we confirmed that these two proteins were polyubiquitinated as well (Fig. 2*A*, *lanes 8* and *4*). On the other hand, Lasp1 (LIM and SH3 protein 1), RGS10 (regulator of G-protein signaling 10), and SOD1 (superoxide dismutase 1), which were identified as proteins with reduced expression in anergized T cells by the two-dimensional difference gel electrophoresis analysis, were not ubiquitinated in the presence of GRAIL (Fig. 2*A*, *lanes 2*, *12*, and *14*). These results indicate that Arp2/3-5 and coronin 1A are selectively polyubiquitinated by GRAIL. Histidine to asparagine substitution in the RING finger domain (H2N2) or deletion of the RING finger domain (ΔRF) of GRAIL (Fig. 2*B*) reportedly inactivates GRAIL. These mutant forms of GRAIL abrogated the ability of GRAIL to ubiquitinate Arp2/3-5 and coronin 1A as well as RhoGDIα and β (Fig. 2*C*). Recent evi-

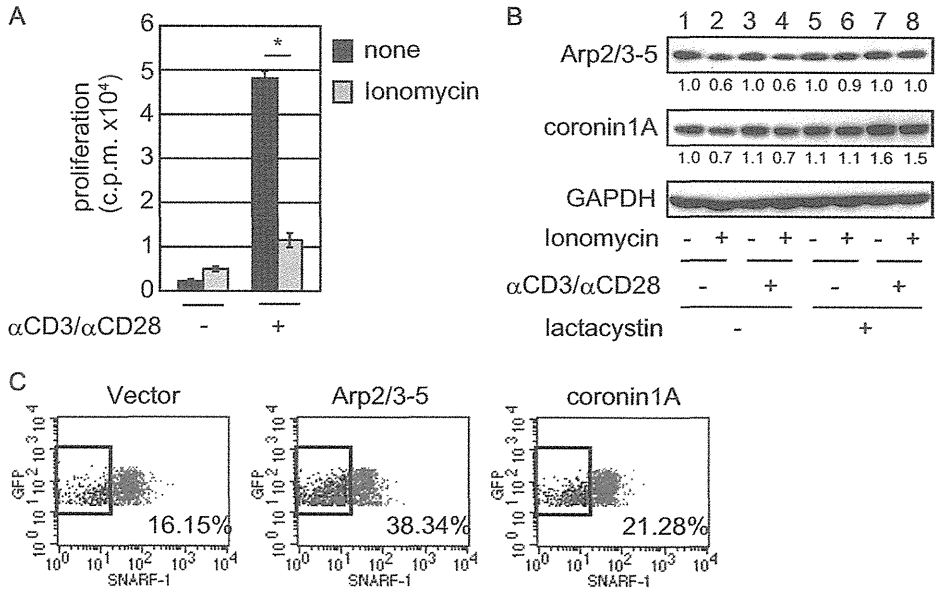

FIGURE 1. **Arp2/3-5 and coronin 1A are down-regulated in T cells anergized by ionomycin.** *A* and *B*, splenocytes derived from DO11.10 mice were stimulated with OVA for 3 days and rested for 7–10 days. The rested T cells were then treated with or without ionomycin for 18 h and restimulated with plate-bound anti-CD3 and soluble anti-CD28. *A*, proliferation was assessed by [^{3}H]thymidine uptake for 48 h. The mean c.p.m. of triplicate wells ± S.E. is shown (n = 9). *, p = 0.0000033 *versus* control. *B*, cells were lysed and analyzed by immunoblotting after 1-hour activation with plate-bound anti-CD3 and soluble anti-CD28. Each protein level analyzed by ImageJ software was normalized to the corresponding GAPDH level and is expressed as relative quantity to that of untreated control. *C*, DO11.10 CD4$^+$ T cells were transfected with vector control (GFP alone), Arp2/3-5, or coronin 1A. Forty-eight hours later, the transfected cells were treated with ionomycin for 18 h and were labeled with SNARF-1. The cells were restimulated with plate-bound anti-CD3 and soluble anti-CD28. Forty-eight hours later, proliferation was analyzed by FACS.

dence suggests that Cbl-b, which is E3 ligase as well as GRAIL, is important for induction of T cell anergy. We also analyzed whether Arp2/3-5 and coronin 1A are substrates of Cbl-b. However, Arp2/3-5 and coronin 1A are not ubiquitinated by Cbl-b (supplemental Fig. S1). These data indicate that GRAIL but not Cbl-b E3 ligase selectively ubiquitinates Arp2/3-5 and coronin 1A.

GRAIL Co-localizes with Arp2/3-5 and Coronin 1A—To address the interaction of Arp2/3-5 and coronin 1A with GRAIL, we examined the co-localization of these proteins. We transiently expressed GFP-tagged GRAIL together with HA-tagged ubiquitin and DsRed-tagged Arp2/3-5, coronin 1A, or RhoDGIα/β. After treatment with lactacystin, the localization of GRAIL and its substrates was analyzed by confocal microscopy. Indeed, Arp2/3-5 (Fig. 3*A*), coronin 1A (Fig. 3*B*), and RhoDGIα and β (Fig. 3, *C* and *D*) all co-localized with GRAIL. The substrates were localized together with GRAIL in contrast to the diffuse localization of GFP and substrate proteins in the cells transfected with GFP control vector and substrate proteins, indicating the co-localization of GRAIL and Arp2/3-5 or coronin 1A. These findings suggest that Arp2/3-5 and coronin 1A interact with GRAIL.

GRAIL Ubiquitinates Arp2/3-5 and Coronin 1A via Lys-63 and Lys-48—GRAIL has been reported to form polyubiquitin chains through lysine 63, resulting in proteolysis-independent functional modulation of Rho GDIs. However, when CD151 is the substrate, polyubiquitin chains are formed through lysine 48, which leads to protein degradation (18). We therefore assessed whether GRAIL ubiquitinates Arp2/3-5 and coronin 1A through Lys-63 and Lys-48. A similar polyubiquitinated ladder pattern of Arp2/3-5 was observed in the presence of WT Ub or Ub containing a lysine to arginine substitution at residue 29 (K29R) (Fig. 4*A*, *lanes 4* and *6*). In contrast, Ub conjugation of Arp2/3-5 was barely detected in the presence of Ub containing a lysine to arginine substitution at residue 48 (K48R) or at residue 63 (K63R) (Fig. 4*A*, *lanes 8* and *10*). Similarly, Ub conjugation of coronin 1A was observed in the presence of WT or K29R Ub (Fig. 4*B*, *lanes 4* and *6*) but was much lower when K48R or K63R Ub was used (Fig. 4*B*, *lanes 8* and *10*). These data reveal that Arp2/3-5 and coronin 1A were modified by Lys-48 and Lys-63 mixed linkage ubiquitin chains. To address the effect of GRAIL on the protein levels of Arp2/3-5 and coronin 1A, we overexpressed GRAIL and its enzymatically inactive mutant, H2N2-GRAIL or ΔRF-GRAIL, in DO11.10 CD4$^+$ T cells and determined Arp2/3-5 and coronin 1A expression by immunoblotting with specific Abs. Both Arp2/3-5 and coronin 1A were reduced when GRAIL, but not the enzymatically inactive forms of GRAIL, was overexpressed (Fig. 4*C*). These results indicate that GRAIL polyubiquitinates Arp2/3-5 and coronin 1A through Lys-48 and Lys-63 and eventually leads them to be degraded.

Less Arp2/3-5 and Coronin 1A Localize at the IS in Anergy—To investigate the role of Arp2/3-5 and coronin 1A in anergic T cells, we next examined the accumulation of F-actin, Arp2/3-5, and coronin 1A at the IS using confocal microscopy. As described previously, F-actin and Arp2/3-5 were recruited to the IS formed between DO11.10 CD4$^+$ T cells and $OVA_{323-339}$ peptide-pulsed A20 B cells (Fig. 5, *A* and *B*, *top panels*). In contrast, the accumulation of F-actin and the recruitment of Arp2/3-5 to the IS were reduced in ionomycin-treated DO11.10 CD4$^+$ T cells compared with those in control cells (Fig. 5*A*, *bottom panel*). Similarly, the recruitment of coronin 1A to the

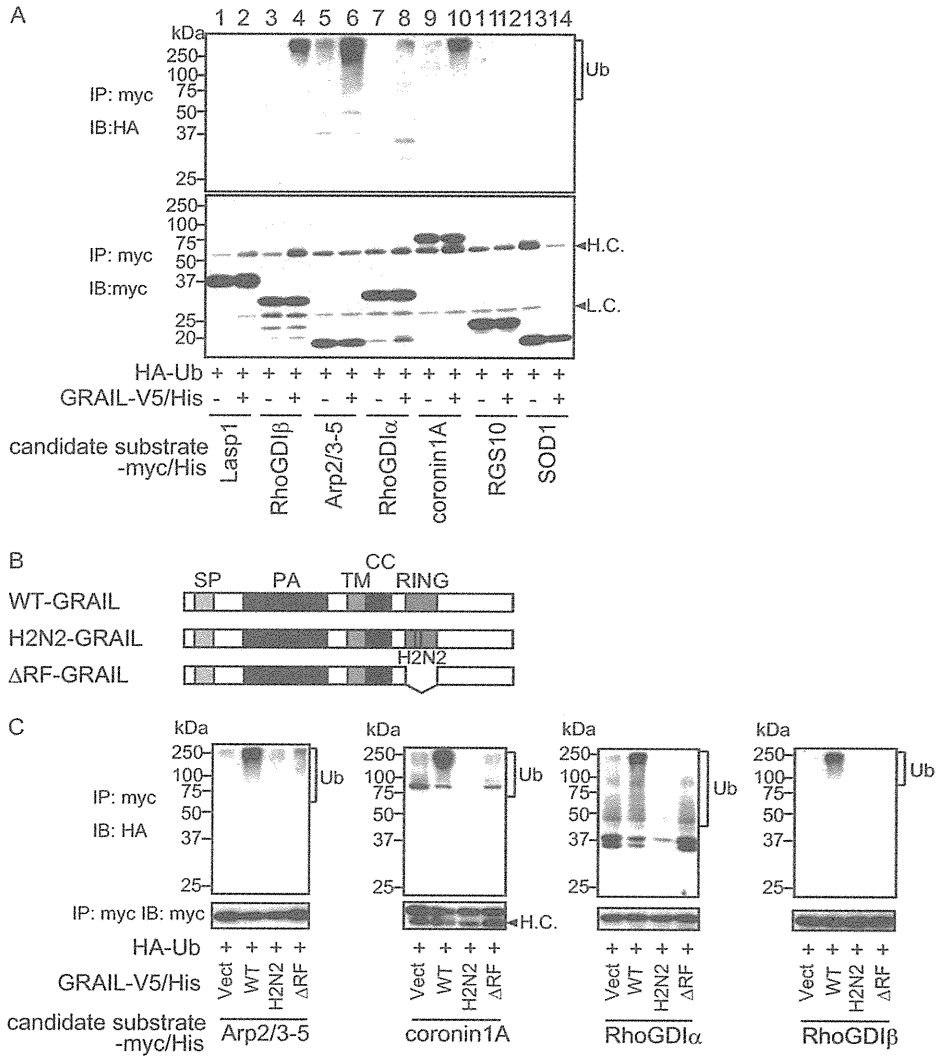

FIGURE 2. **Arp2/3-5 and coronin 1A are ubiquitinated by GRAIL.** *A* and *C*, HEK293T cells were transiently transfected with the indicated constructs and were treated with lactacystin for 12 h before lysis. Ubiquitination of the indicated proteins was detected by immunoprecipitation (*IP*) with anti-Myc Ab, followed by anti-HA immunoblotting (*IB*). The membrane was stripped and reprobed with anti-Myc Ab. *B*, schematic structures of the WT-, H2N2-, and ΔRF-GRAIL proteins.

IS in ionomycin-treated DO11.10 $CD4^+$ T cells was reduced compared with that in nontreated DO11.10 $CD4^+$ T cells (Fig. 5*B*, *bottom panel*). These data demonstrate that the accumulation of Arp2/3-5 and coronin 1A together with F-actin at the IS is impaired in anergic T cells.

GRAIL Inhibits Arp2/3 and Coronin 1A Accumulation at the IS—To address the contribution of GRAIL to IS formation, we overexpressed GRAIL, ΔRF-GRAIL, or a control vector in DO11.10 $CD4^+$ T cells and analyzed the accumulation of Arp2/3-5, coronin 1A, and F-actin at the IS. First, the expression of Arp2/3-5 and coronin 1A was reduced in T cells (GFP-positive cells) in which GRAIL was overexpressed compared with expression levels in control cells (Fig. 6, *A* and *B*, compare *top* and *middle panels*). The accumulation of both Arp2/3-5 and coronin 1A together with F-actin was reduced in DO11.10 $CD4^+$ T cells overexpressing GRAIL compared with that in control vector-transfected T cells (Fig. 6, *A* and *B*, compare *top* and *middle panels*). On the other hand, the accumulation of Arp2/3-5, coronin 1A, and F-actin at the IS in DO11.10 $CD4^+$ T cells overexpressing ΔRF-GRAIL was similar to that in controls (Fig. 6, *A* and *B*, *bottom panels*). We also examined whether the formation of IS occurred in ionomycin-treated T cells in which GRAIL was down-regulated by GRAIL shRNA-encoding retroviral infection. Coincident with the results for GRAIL-overexpressing experiments, both Arp2/3–5 and coronin 1A together with F-actin fully accumulated at the IS in ionomycin-treated GRAIL knockdown DO11.10 $CD4^+$ T cells compared with that in ionomycin-treated control T cells (anergic T cells) (supplemental Fig. S2). These results indicated that GRAIL regulates the recruitment of Arp2/3-5 and coronin 1A into the IS and the subsequent accumulation of F-actin at the site of the IS.

GRAIL Inhibits Lamellipodium Formation—Because Arp2/3 has been reported to be essential for the formation of lamellipodia at the IS, we next examined the effect of GRAIL on lamellipodium formation. Because the spreading of T cells on anti-TCR-coated coverslips requires the formation of stable actin structures and the generation of lamellipodia, we first analyzed whether T cells could spread onto anti-CD3-coated coverslips

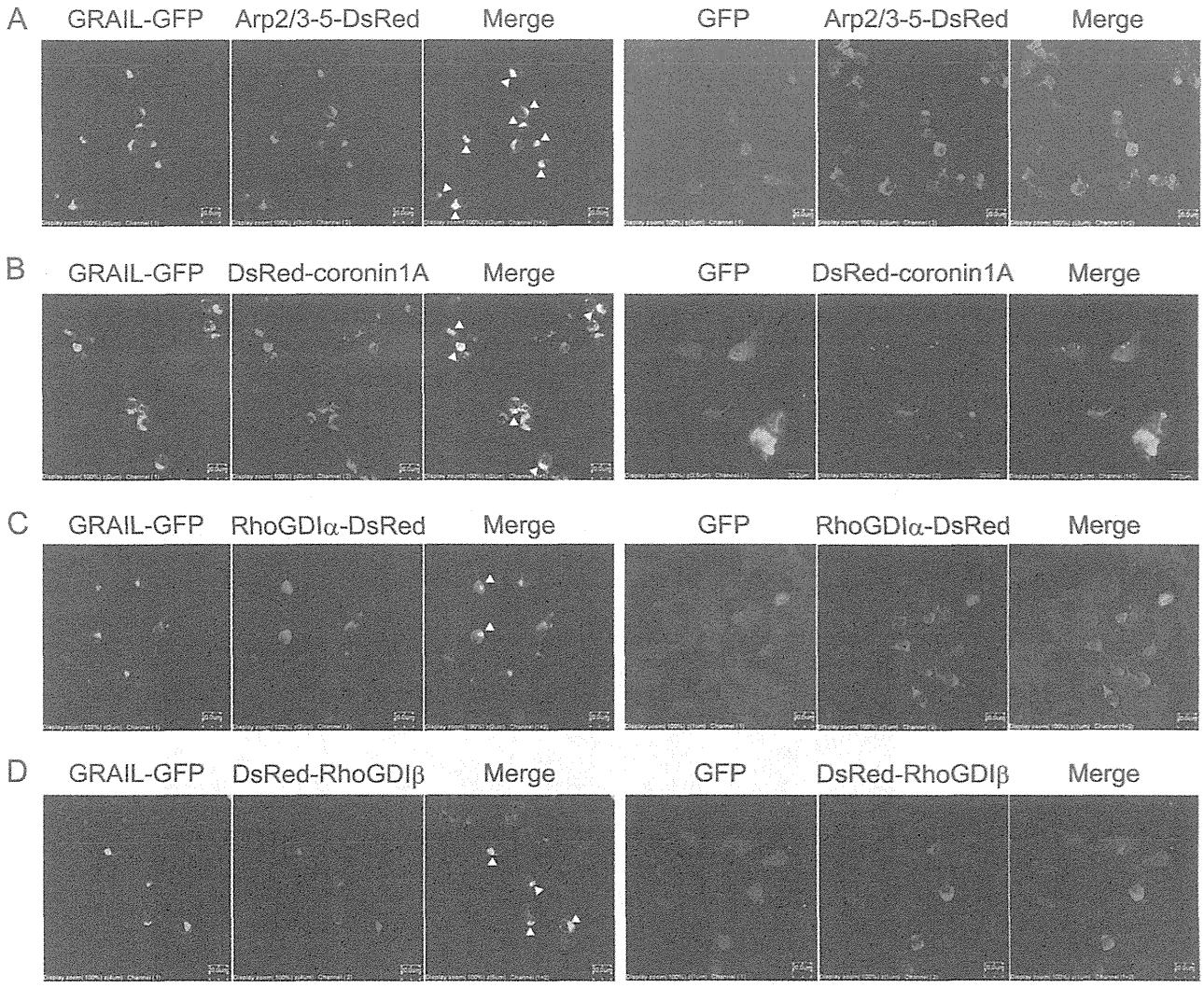

FIGURE 3. **GRAIL co-localizes with Arp2/3-5 and coronin 1A.** HEK293T cells were transiently transfected with constructs expressing GFP-tagged GRAIL, DsRed-tagged substrates (Arp2/3-5, *A*; coronin1A, *B*; RhoGDIα, *C*, and RhoGDIβ, *D*), and HA-ubiquitin and were treated with lactacystin for 12 h before being fixed. Co-localization with GFP-GRAIL was analyzed by confocal microscopy.

under anergic conditions. Control DO11.10 $CD4^+$ T cells spread onto anti-TCR-coated coverslips and formed round lamellipodial interfaces containing F-actin-rich structures (Fig. 7*A*). In contrast, DO11.10 $CD4^+$ T cells in which anergy had been induced by ionomycin barely formed lamellipodia (Fig. 7*A*, *bottom panels*). We next analyzed the lamellipodium formation in $CD4^+$ T cells overexpressing GRAIL. Lamellipodia were not efficiently formed on anti-CD3-coated coverslips when GRAIL was overexpressed in DO11.10 $CD4^+$ T cells (Fig. 7*B*, *middle panels*). In contrast, lamellipodia were efficiently formed at the IS when a catalytically inactive mutant GRAIL (ΔRF) was overexpressed in DO11.10 $CD4^+$ T cells (Fig. 7*B*, *bottom panels*). These data demonstrate that GRAIL inhibits lamellipodium formation at the IS.

DISCUSSION

In this study, we demonstrate that Arp2/3-5 and coronin 1A are down-regulated in anergic T cells as well as in T cells that overexpress GRAIL. Arp2/3-5 and coronin 1A co-localize with GRAIL and are ubiquitinated by GRAIL but not by Cbl-b via Lys-48 and Lys-63 linkage. Furthermore, the accumulation of Arp2/3-5 and coronin 1A together with F-actin is reduced at the IS in anergic T cells or in T cells that overexpress GRAIL. Coincident with the results for GRAIL-overexpressing experiments, IS formation in ionomycin-treated anergic T cells occurred by knockdown of GRAIL. Finally, we showed that overexpression of GRAIL suppresses lamellipodium formation at the IS.

CD40 ligand, CD151, CD83, and RhoGDI have been reported to be candidate substrates of GRAIL; however, the mechanism of GRAIL-mediated anergy induction is not yet fully understood (18–21). In fact, the expression of CD40 ligand was not up-regulated, and the down-regulation of CD3 was impaired in GRAIL-deficient mice. Because GRAIL is the only membrane protein among E3 ligases up-regulated in anergic T cells, it is reasonable that membrane proteins such as CD151 or CD83 are regulated by GRAIL. In this study, we confirmed that cytosolic proteins such as RhoGDIs serve as substrates for GRAIL. Fur-

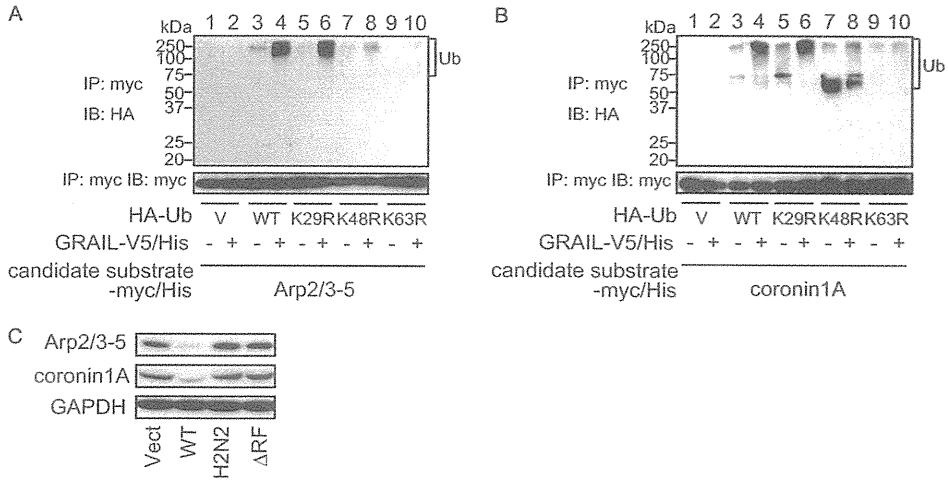

FIGURE 4. **Arp2/3-5 and coronin 1A are polyubiquitinated though Lys-48 and/or Lys-63 ubiquitin linkages and are down-regulated by catalytically active GRAIL.** *A* and *B*, HEK293T cells were transiently transfected with the indicated vectors and were treated with lactacystin for 12 h before lysis. Arp2/3-5 (*A*) and coronin 1A (*B*) were immunoprecipitated (*IP*) with anti-Myc Ab followed by immunoblotting (*IB*) with anti-HA Ab. The membrane was stripped and reprobed with anti-Myc Ab. *C*, $CD4^+$ T cells were transfected with vector control (GFP alone) or WT-, H2N2-, or ΔRF-GRAIL expression constructs. Forty-eight hours later, the transfected cells (GFP^+ cells) were sorted using a FACS Aria cell sorter. Sorted cells were rested for 2 days and were subjected to immunoblot analysis with anti-coronin 1A or Arp2/3-5 Ab.

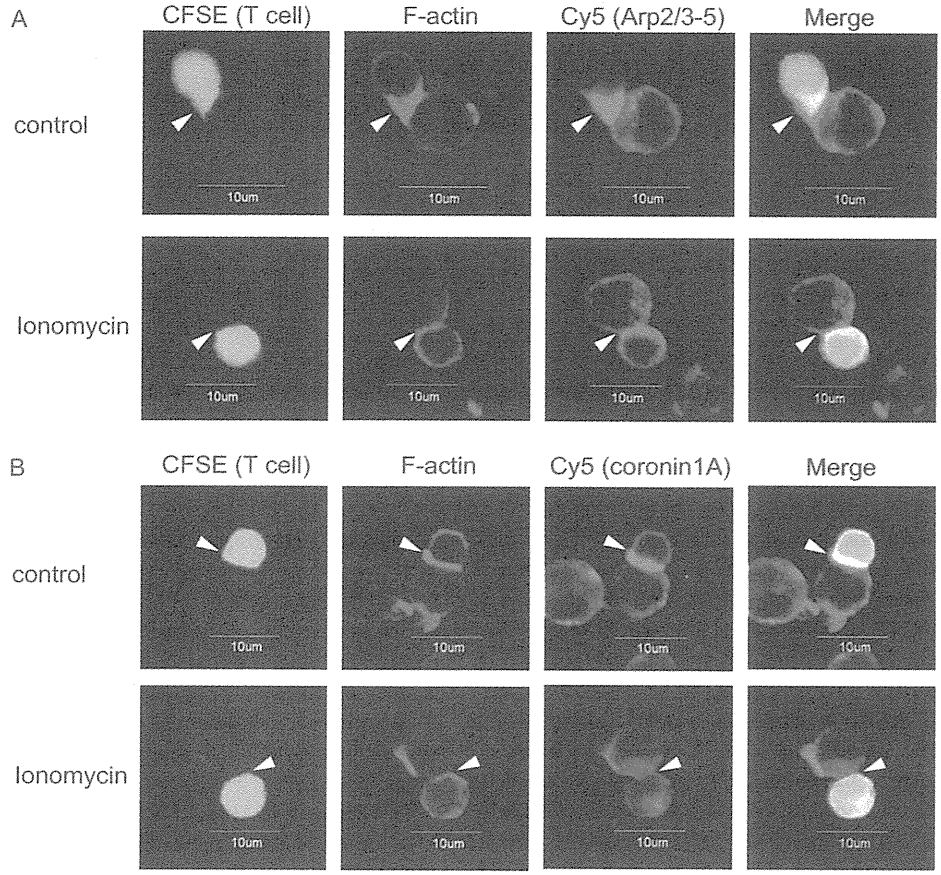

FIGURE 5. **The accumulation of Arp2/3-5, coronin 1A, and F-actin at the IS is reduced in anergic T cells.** *A* and *B*, OVA-stimulated DO11.10 splenocytes were rested for 7–10 days. Rested T cells were stained with CFSE, treated with or without ionomycin for 18 h, incubated with $OVA_{323-339}$-pulsed A20 cells, and co-stained with rhodamine-phalloidin (*red*) to visualize F-actin and either anti-Arp2/3-5 Ab (*A*) or anti-coronin 1A Ab (*purple*) (*B*). The *arrowheads* indicate IS.

thermore, we identified Arp2/3-5 and coronin 1A as novel substrates for GRAIL. Interestingly, these proteins as well as RhoGDIs are reportedly involved in the regulation of cytoskeletal organization. Although ubiquitination of target proteins was almost completely lost when either K63R or K48R mutant ubiquitin was used, it remains unclear whether Arp2/3-5 and coronin 1A are ubiquitinated via Lys-48, Lys-63, or both sites. To address this issue, characterization of ubiquitin chain using

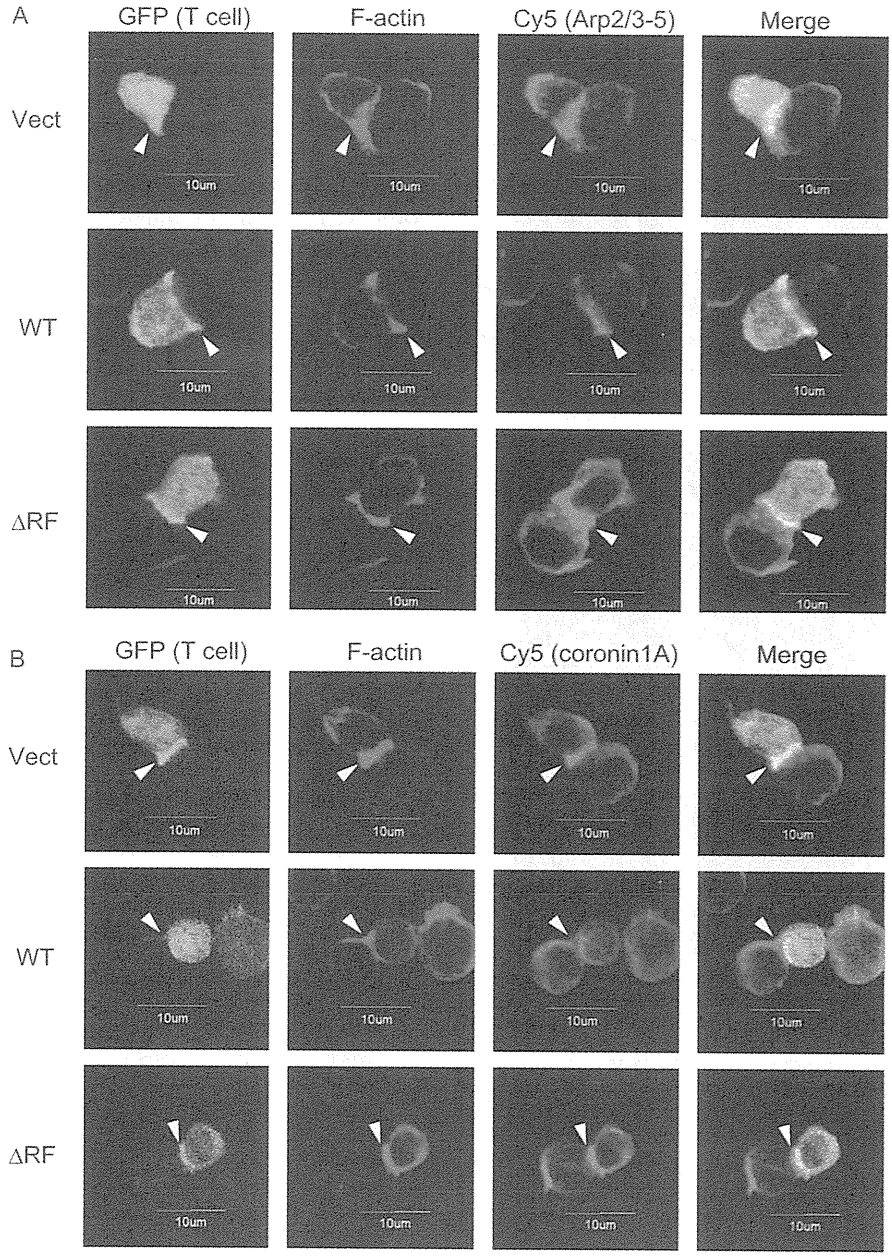

FIGURE 6. **GRAIL inhibits the accumulation of Arp2/3-5, coronin 1A, and F-actin at the IS.** *A* and *B*, DO11.10 $CD4^+$ T cells were transfected with vector control (GFP alone) or WT- or ΔRF-GRAIL expression constructs (*green*). Each population was incubated with $OVA_{323-339}$-pulsed A20 cells and co-stained with rhodamine-phalloidin (*red*) and either anti-Arp2/3-5 (*A*) or anti-coronin 1A (*purple*) (*B*). The *arrowheads* indicate IS.

MALDI-TOF-MS or mutants in which Lys-48 or Lys-63 is the only lysine residue that can mediate the ubiquitin chain formation will be needed for future studies

The immunological synapse is important in sustained signaling and delivery of a subset of effector cytokines by $CD4^+$ T cells (25, 29, 31, 32). Although the precise contribution of actin cytoskeletal remodeling to T cell signaling and biologic function is not completely understood, both anergic T cells and T cells overexpressing GRAIL have been reported to form unstable immunologic synapses (4, 38). Actin nucleation in T cells is induced by the WAVE2 complex (33) and the actin-nucleation-promoting factor WASPs, which are required to promote and stabilize interactions between T cells and APC *in vitro* and TCR clustering on artificial surfaces. WASPs bind to actin monomers, whereas the acidic stretch associates with the Arp2/3-5 complex (23, 34), a seven-subunit complex that has intrinsic actin-nucleating activity and is essential for polarization of F-actin at the IS (25, 35). In addition, co-localization of WASPs and the Arp2/3-5 complex at the interface between anti-CD3-coated beads and Jurkat T cells suggests that these cytoskeletal components are essential for the dynamics of the actin cytoskeleton and for T cell function (24). Arp2/3-5 is essential for the formation of a stable synapse by creating lamellipodia (25). Consistent with these findings, overexpression of GRAIL reduced the protein expression of Arp2/3-5 and impaired lamellipodium formation. These results suggest that proteins

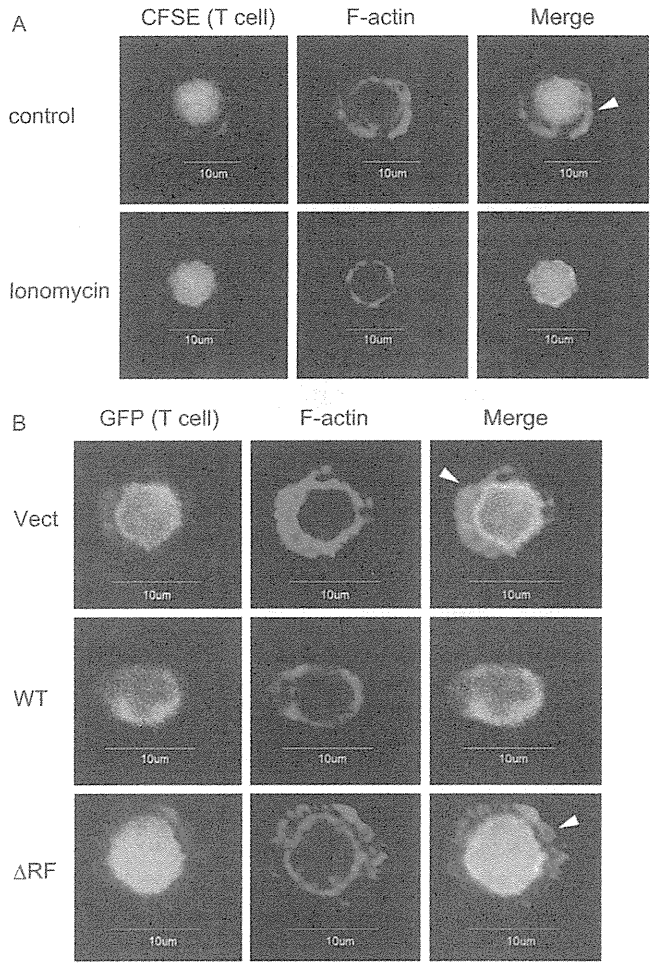

FIGURE 7. **GRAIL inhibits lamellipodium formation during TCR stimulation.** *A*, OVA-stimulated DO11.10 splenocytes were rested for 7–10 days and stained with CFSE. The cells were treated with or without ionomycin for 18 h. The cells were stimulated with plate-bound anti-CD3 mAb and stained with rhodamine-phalloidin (*red*) to visualize F-actin. *B*, DO11.10 $CD4^+$ T cells were transfected with a control vector (GFP alone) or WT- or ΔRF-GRAIL expression vectors. The cells were stimulated with coated anti-CD3 mAb and stained with rhodamine-phalloidin (*red*). The *arrowheads* indicate lamellipodium formation.

related to cytoskeletal reorganization at the IS are cytosolic targets for GRAIL.

An earlier study of coronin 1A knock-out mice reported that coronin 1A has an Arp2/3-5-dependent inhibitory effect on F-actin formation and concluded that coronin 1A is indispensable for TCR signaling (27, 29). In the present study, overexpression of coronin 1A restored the proliferative response. These findings suggest that coronin 1A participates in modulating T cell signaling and thereby contributes to the maintenance of anergy. In anergic T cells and in T cells overexpressing GRAIL, F-actin accumulation at the IS was decreased, although the expression of coronin 1A was reduced in contrast to previous studies. This may be because GRAIL regulates not only coronin 1A but also the Arp2/3-5 complex as well as RhoGDIs, which are important in the regulation of the accumulation of F-actin.

Anergic T cells have been reported to exhibit initial interaction, but implementation of T cell anergy results in reduced binding of LFA-1 to its ligand ICAM-1 (4). This process is mediated through degradation of PKC-θ and phospholipase C-γ by Cbl-b. A recent report demonstrated that overexpression of GRAIL impairs LFA-1 polarization at the IS (37). Stimulation through the TCR was shown to result in WAVE2-Arp2/3-5-dependent F-actin nucleation and the formation of a complex containing WAVE2, Arp2/3-5, vinculin, and talin (33). Moreover, TCR stimulation induces integrin clustering through the recruitment of vinculin and talin (33). Therefore, our study might link the unstable immunological synapse formation and impaired LFA-1 polarization at the IS in anergic T cells. Thus, whereas Cbl-b leads to unstable immunological synapse through degradation of tyrosine kinase, GRAIL leads to the phenotype of synapse disorganization via degradation of proteins involved in the actin cytoskeletal organization. In summary, we provide evidence that GRAIL regulates cytoskeletal reorganization to keep cells unresponsive to further antigen stimulation through the ubiquitination and down-regulation of the Arp2/3-5 complex and coronin 1A.

REFERENCES

1. Schwartz, R. H. (2003) *Annu. Rev. Immunol.* **21,** 305–334
2. Walker, L. S., and Abbas, A. K. (2002) *Nat. Rev. Immunol.* **2,** 11–19
3. Quill, H., and Schwartz, R. H. (1987) *J. Immunol.* **138,** 3704–3712
4. Heissmeyer, V., Macián, F., Im, S. H., Varma, R., Feske, S., Venuprasad, K., Gu, H., Liu, Y. C., Dustin, M. L., and Rao, A. (2004) *Nat. Immunol.* **5,** 255–265
5. Jeon, M. S., Atfield, A., Venuprasad, K., Krawczyk, C., Sarao, R., Elly, C., Yang, C., Arya, S., Bachmaier, K., Su, L., Bouchard, D., Jones, R., Gronski, M., Ohashi, P., Wada, T., Bloom, D., Fathman, C. G., Liu, Y. C., and Penninger, J. M. (2004) *Immunity* **21,** 167–177
6. Venuprasad, K., Elly, C., Gao, M., Salek-Ardakani, S., Harada, Y., Luo, J. L., Yang, C., Croft, M., Inoue, K., Karin, M., and Liu, Y. C. (2006) *J. Clin. Invest.* **116,** 1117–1126
7. Hsiao, H. W., Liu, W. H., Wang, C. J., Lo, Y. H., Wu, Y. H., Jiang, S. T., and Lai, M. Z. (2009) *Immunity* **31,** 72–83
8. Anandasabapathy, N., Ford, G. S., Bloom, D., Holness, C., Paragas, V., Seroogy, C., Skrenta, H., Hollenhorst, M., Fathman, C. G., and Soares, L. (2003) *Immunity* **18,** 535–547
9. Andoniou, C. E., Lill, N. L., Thien, C. B., Lupher, M. L., Jr., Ota, S., Bowtell, D. D., Scaife, R. M., Langdon, W. Y., and Band, H. (2000) *Mol. Cell Biol.* **20,** 851–867
10. Rao, N., Miyake, S., Reddi, A. L., Douillard, P., Ghosh, A. K., Dodge, I. L., Zhou, P., Fernandes, N. D., and Band, H. (2002) *Proc. Natl. Acad. Sci. U.S.A.* **99,** 3794–3799
11. Lupher, M. L., Jr., Rao, N., Lill, N. L., Andoniou, C. E., Miyake, S., Clark, E. A., Druker, B., and Band, H. (1998) *J. Biol. Chem.* **273,** 35273–35281
12. Lupher, M. L., Jr., Songyang, Z., Shoelson, S., Cantley, L. C., and Band, H. (1997) *J. Biol. Chem.* **272,** 33140–33144
13. Duan, L., Reddi, A. L., Ghosh, A., Dimri, M., and Band, H. (2004) *Immunity* **21,** 7–17
14. Fang, D., and Liu, Y. C. (2001) *Nat. Immunol.* **2,** 870–875
15. Liu, Y. C. (2004) *Annu. Rev. Immunol.* **22,** 81–127
16. Kriegel, M. A., Rathinam, C., and Flavell, R. A. (2009) *Proc. Natl. Acad. Sci. U.S.A.* **106,** 16770–16775
17. Nurieva, R. I., Zheng, S., Jin, W., Chung, Y., Zhang, Y., Martinez, G. J., Reynolds, J. M., Wang, S. L., Lin, X., Sun, S. C., Lozano, G., and Dong, C. (2010) *Immunity* **32,** 670–680
18. Lineberry, N. B., Su, L. L., Lin, J. T., Coffey, G. P., Seroogy, C. M., and Fathman, C. G. (2008) *J. Immunol.* **181,** 1622–1626
19. Lineberry, N., Su, L., Soares, L., and Fathman, C. G. (2008) *J. Biol. Chem.* **283,** 28497–28505
20. Su, L. L., Iwai, H., Lin, J. T., and Fathman, C. G. (2009) *J. Immunol.* **183,** 438–444

21. Su, L., Lineberry, N., Huh, Y., Soares, L., and Fathman, C. G. (2006) *J. Immunol.* **177,** 7559–7566
22. Holsinger, L. J., Graef, I. A., Swat, W., Chi, T., Bautista, D. M., Davidson, L., Lewis, R. S., Alt, F. W., and Crabtree, G. R. (1998) *Curr. Biol.* **8,** 563–572
23. Machesky, L. M., and Insall, R. H. (1998) *Curr. Biol.* **8,** 1347–1356
24. Krause, M., Sechi, A. S., Konradt, M., Monner, D., Gertler, F. B., and Wehland, J. (2000) *J. Cell Biol.* **149,** 181–194
25. Gomez, T. S., Kumar, K., Medeiros, R. B., Shimizu, Y., Leibson, P. J., and Billadeau, D. D. (2007) *Immunity* **26,** 177–190
26. Nolz, J. C., Gomez, T. S., Zhu, P., Li, S., Medeiros, R. B., Shimizu, Y., Burkhardt, J. K., Freedman, B. D., and Billadeau, D. D. (2006) *Curr. Biol.* **16,** 24–34
27. Föger, N., Rangell, L., Danilenko, D. M., and Chan, A. C. (2006) *Science* **313,** 839–842
28. Rodal, A. A., Sokolova, O., Robins, D. B., Daugherty, K. M., Hippenmeyer, S., Riezman, H., Grigorieff, N., and Goode, B. L. (2005) *Nat. Struct. Mol. Biol.* **12,** 26–31
29. Mugnier, B., Nal, B., Verthuy, C., Boyer, C., Lam, D., Chasson, L., Nieoullon, V., Chazal, G., Guo, X. J., He, H. T., Rueff-Juy, D., Alcover, A., and Ferrier, P. (2008) *PLos One.* **3,** e3467
30. Haraldsson, M. K., Louis-Dit-Sully, C. A., Lawson, B. R., Sternik, G., Santiago-Raber, M. L., Gascoigne, N. R., Theofilopoulos, A. N., and Kono, D. H. (2008) *Immunity.* **28,** 40–51
31. Bachmaier, K., Krawczyk, C., Kozieradzki, I., Kong, Y. Y., Sasaki, T., Oliveira-dos-Santos, A., Mariathasan, S., Bouchard, D., Wakeham, A., Itie, A., Le, J., Ohashi, P. S., Sarosi, I., Nishina, H., Lipkowitz, S., and Penninger, J. M. (2000) *Nature.* **403,** 211–216
32. Fang, D., Wang, H. Y., Fang, N., Altman, Y., Elly, C., and Liu, Y. C. (2001) *J. Biol. Chem.* **276,** 4872–4878
33. Nolz, J. C., Medeiros, R. B., Mitchell, J. S., Zhu, P., Freedman, B. D., Shimizu, Y., and Billadeau, D. D. (2007) *Mol. Cell Biol.* **27,** 5986–6000
34. Miki, H., Miura, K., and Takenawa, T. (1996) *EMBO J.* **15,** 5326–5335
35. Goley, E. D., and Welch, M. D. (2006) *Nat. Rev. Mol. Cell Biol.* **7,** 713–726
36. Deleted in proof
37. Schartner, J. M., Simonson, W. T., Wernimont, S. A., Nettenstrom, L. M., Huttenlocher, A., and Seroogy, C. M. (2009) *J. Biol. Chem.* **284,** 34674–34681
38. Mueller, P., Massner, J., Jayachandran, R., Combaluzier, B., Albrecht, I., Gatfield, J., Blum, C., Ceredig, R., Rodewald, H. R., Rolink, A. G., and Pieters, J. (2008) *Nat. Immunol.* **9,** 424–431